Power and Particle Control

Can fusion power be handled by surrounding wall?

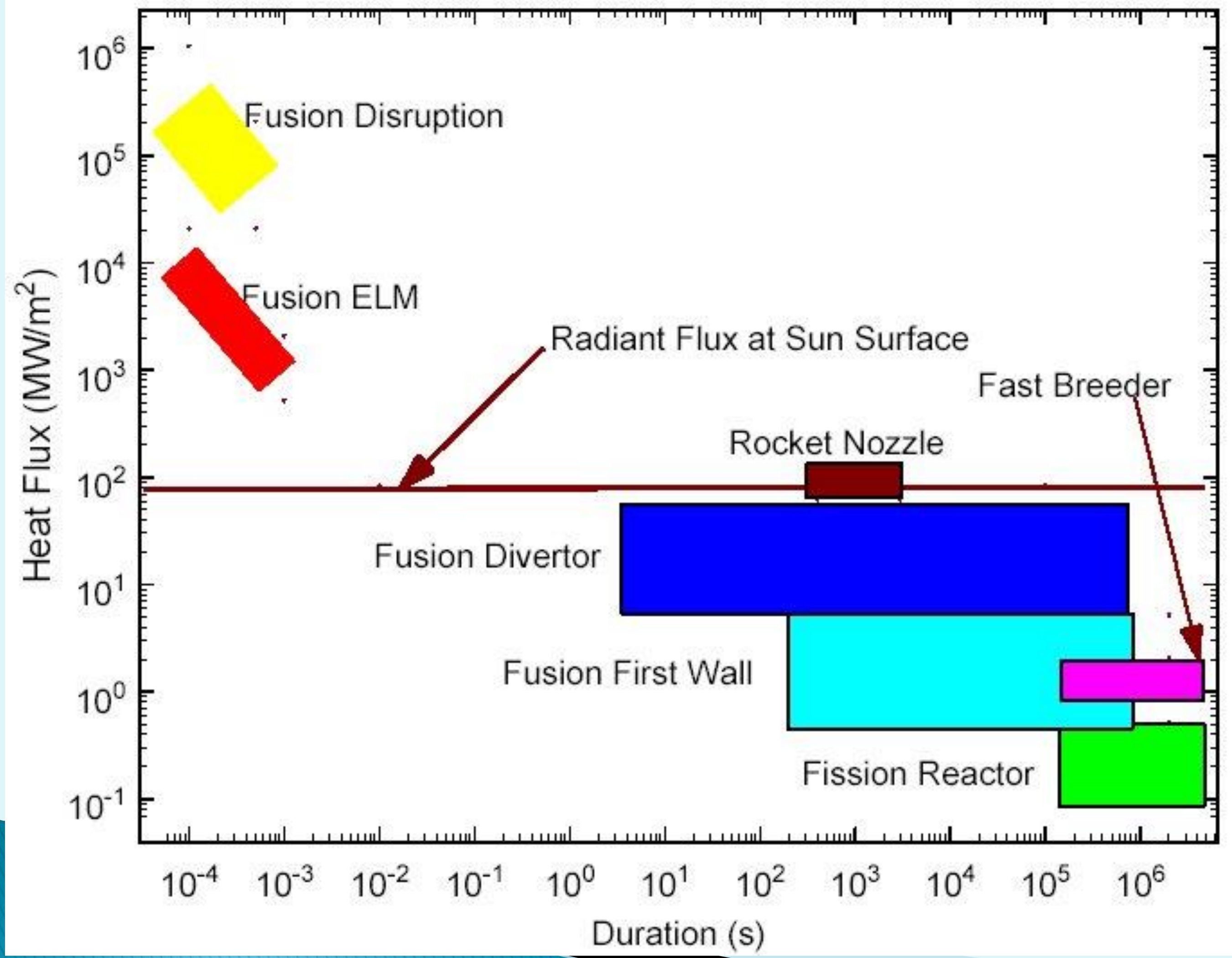

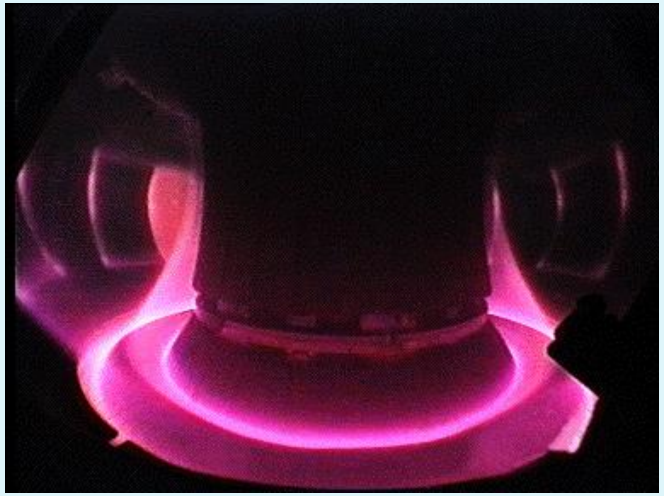

Divertor Heat Load

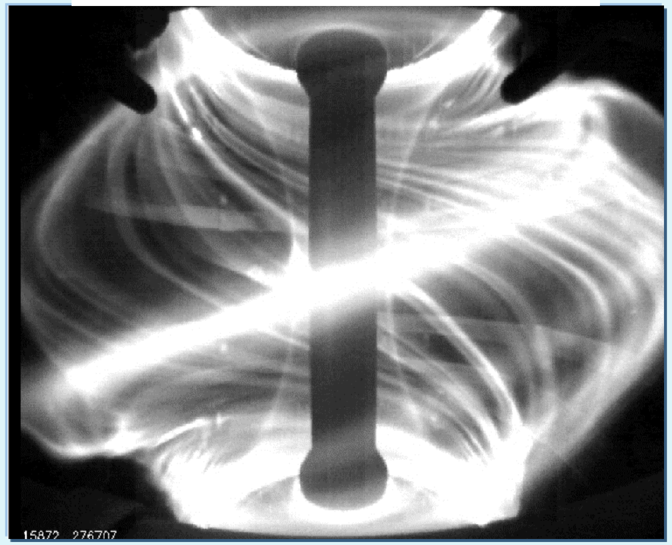

ELM(Edge Localized Mode)

Steady-state transport in the Scrape-Off-Layer (SOL)

ITER

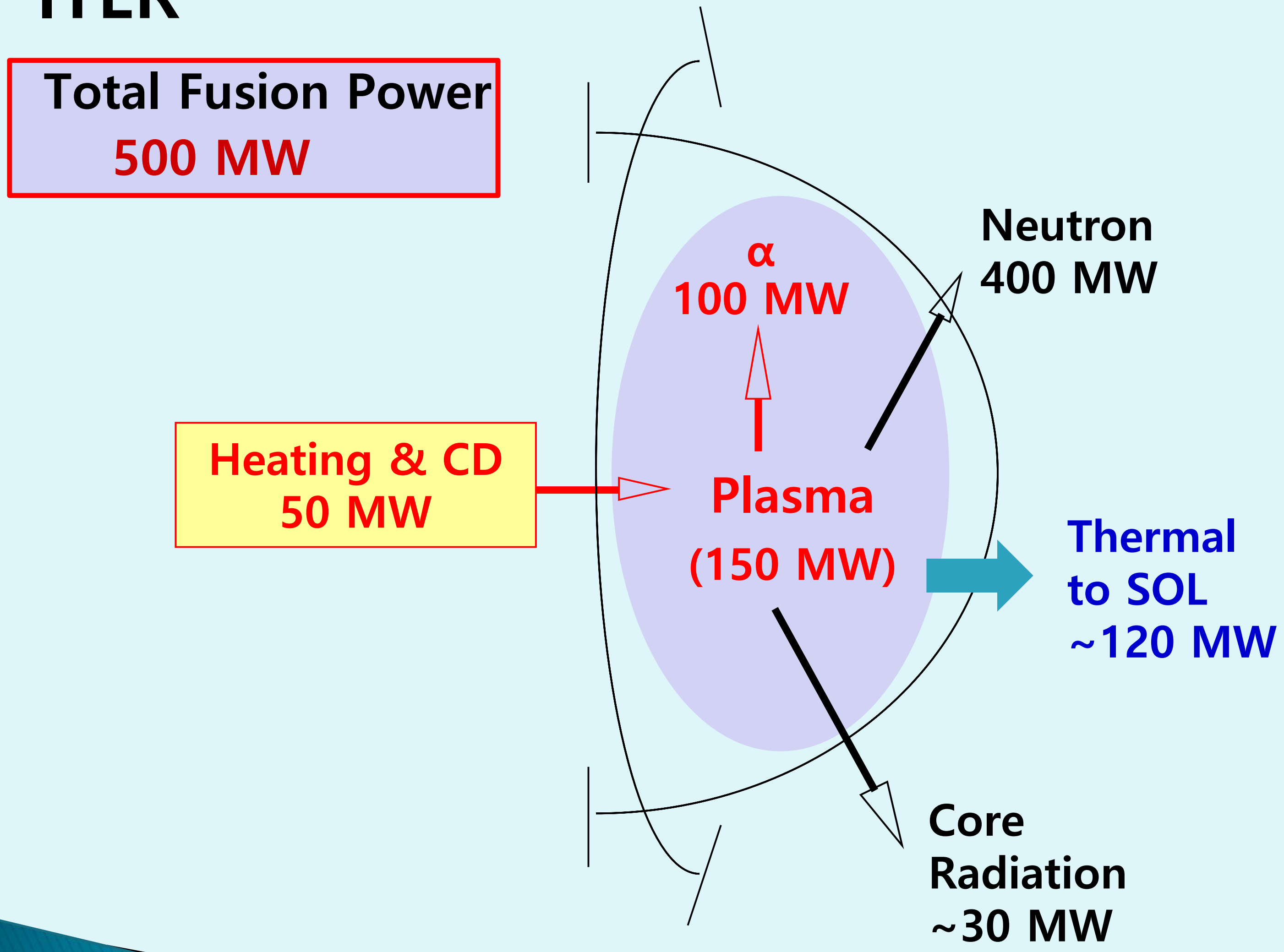

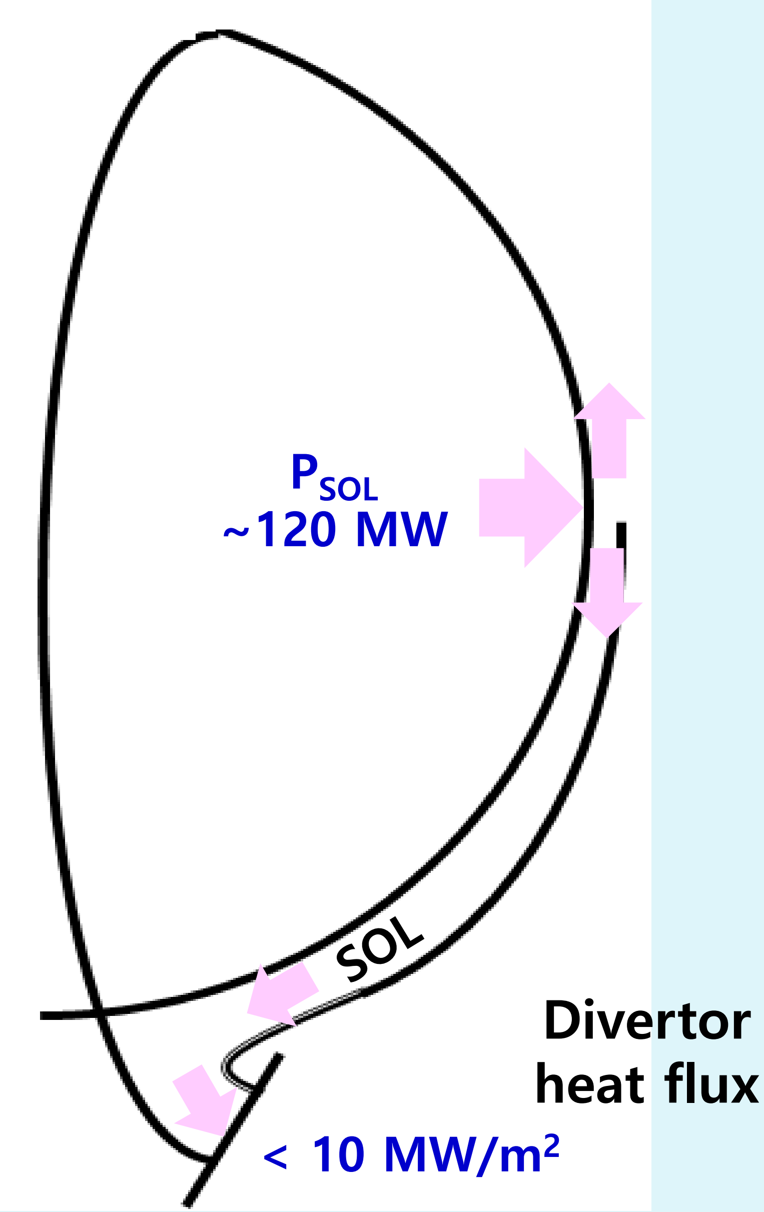

Can fusion power be handled by surrounding wall?

Divertor heat flux

$q_{pol} \rightarrow q_{\parallel} \rightarrow q_{\perp,target}$

Geometry: field pitch,
flux expansion,
target plate tilting

- Peak poloidal heat flux $$q_{pol} \sim \frac{P_{SOL}/2}{2pRl_q}$$
- Parallel heat flux $$q_{\parallel} \sim \frac{P_{SOL}/2}{2pRl_q}\frac{B}{B_q}$$
- Target heat flux $$Area \sim 2\pi R\lambda_q (B_\theta/B)_u / \sin(\alpha)(B_\theta/B)_t$$

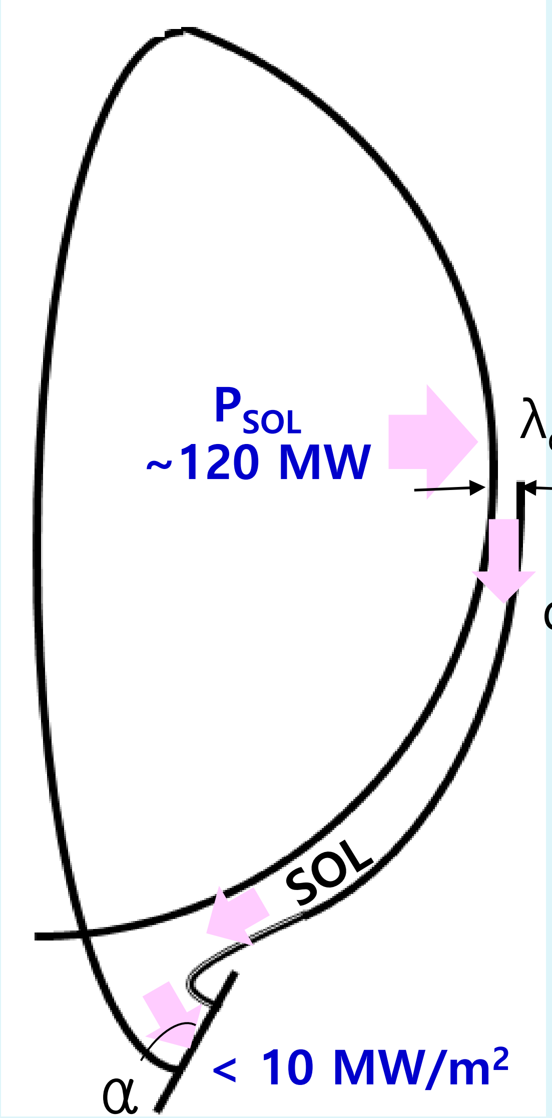

Divertor Heat Flux Challenge with Short SOL Width

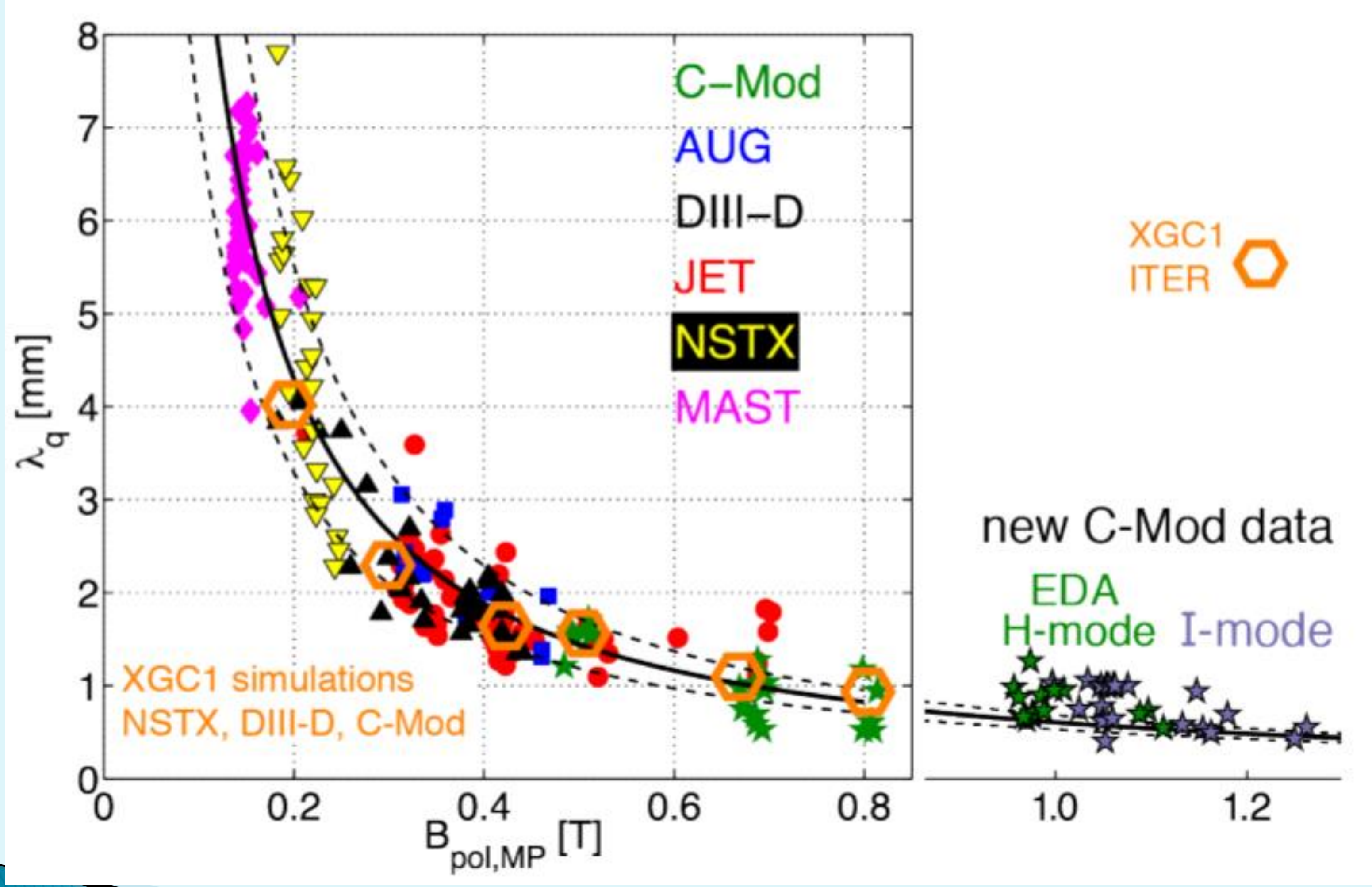

D. Brunner et al., 2017APS-DPP

Can fusion power be handled by surrounding wall?

Increasing core radiation

Assume f_{LH} = 1.2 for ITER, f_{LH} = 1.1 for EU-DEMO, λ_q = 5 cm on the target for both

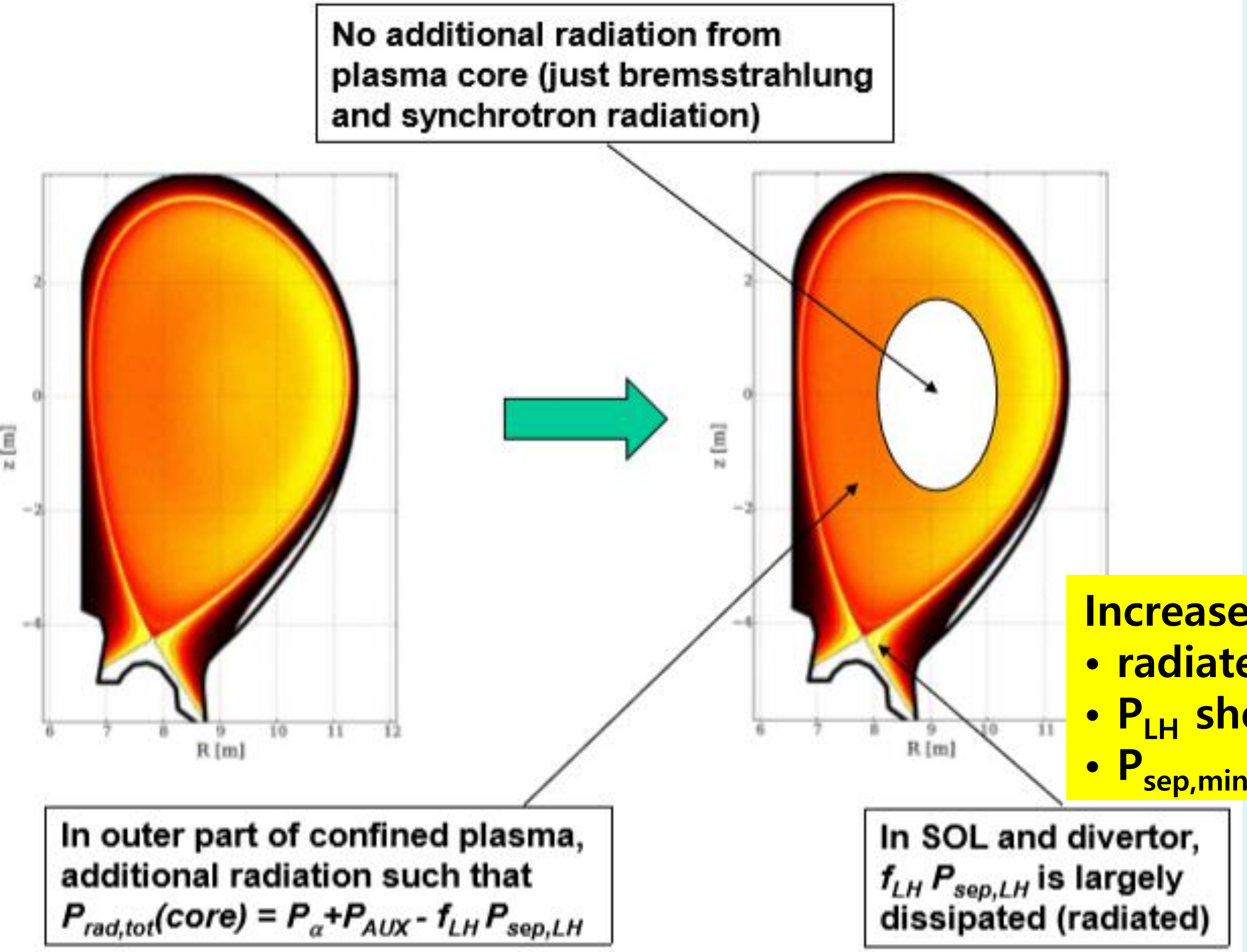

	ITER	EU-DEMO
R [m]	6.2	8.5
P_{fus} [MW]	500	2500
P_{heat} [MW]	150	550
P_{sep} [MW]	85	120
$f_{rad,core}$	43%	78%

Increase the radiated power fraction in the core

- **radiated power limited by the need to stay in H-mode**
- **P_{LH} should be expressed in $P_{sep} = P_{heat} - P_{rad}$**
- **$P_{sep,min} = f_{LH} P_{sep,LH} \propto n_e^{0.7} B_t^{0.8} R^2$**

Zohm, H., *Physics of divertor power exhaust beyond ITER*, 10th ITER international school 2019.

Can fusion power be handled by surrounding wall?

Divertor heat flux reduction

- increasing core radiation
- **Detachment and radiation cooling**

Partially detached (CX-ES limited):
n_t decreases, T_t < 5 eV, $p_t \ll p_u$

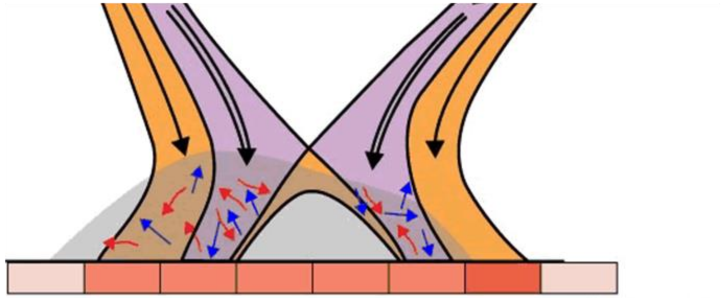

Fully detached (radiation limited):
X-point MARFE

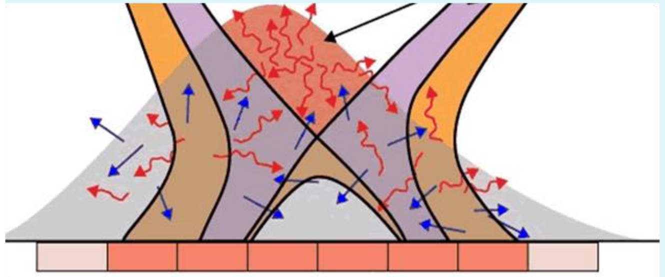

- **Various configurations**
  - X, Super X (**SX**), SnowFlake (**SF**), Double Null (**DN**), …

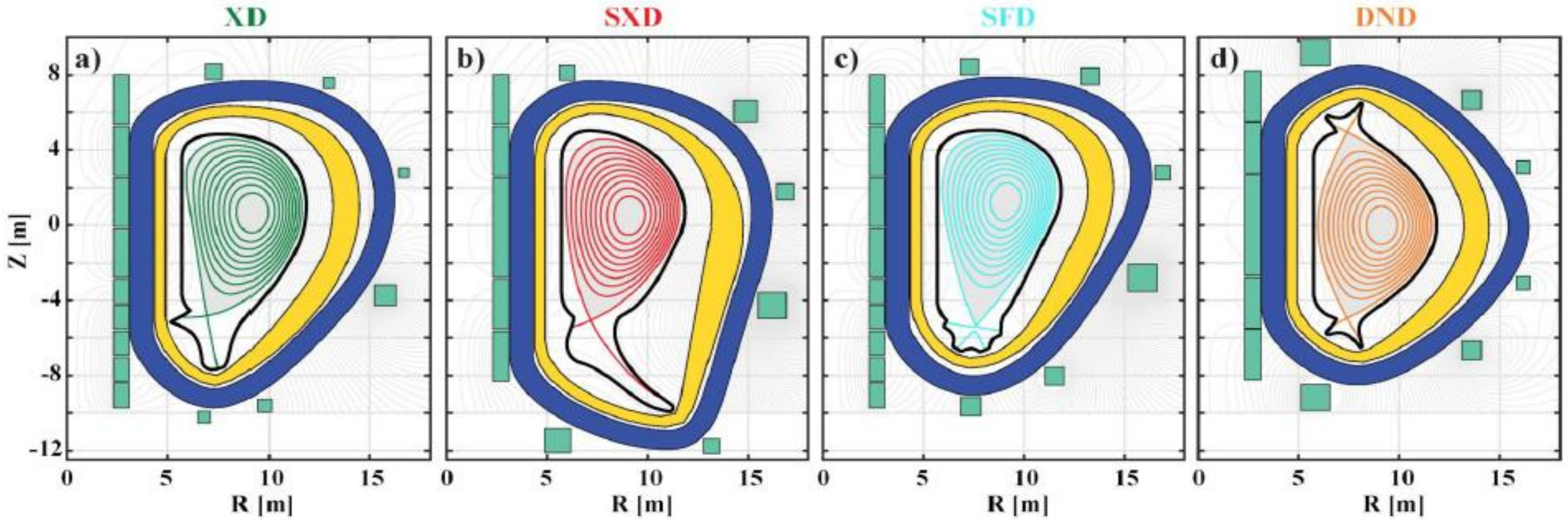

- **Liquid Li**

Zohm, H., *Physics of divertor power exhaust beyond ITER*, 10th ITER international school 2019.

Can fusion power be handled by surrounding wall?

Liquid Lithium: Alternative (liquid) materials may lead to higher allowable P_{sep}

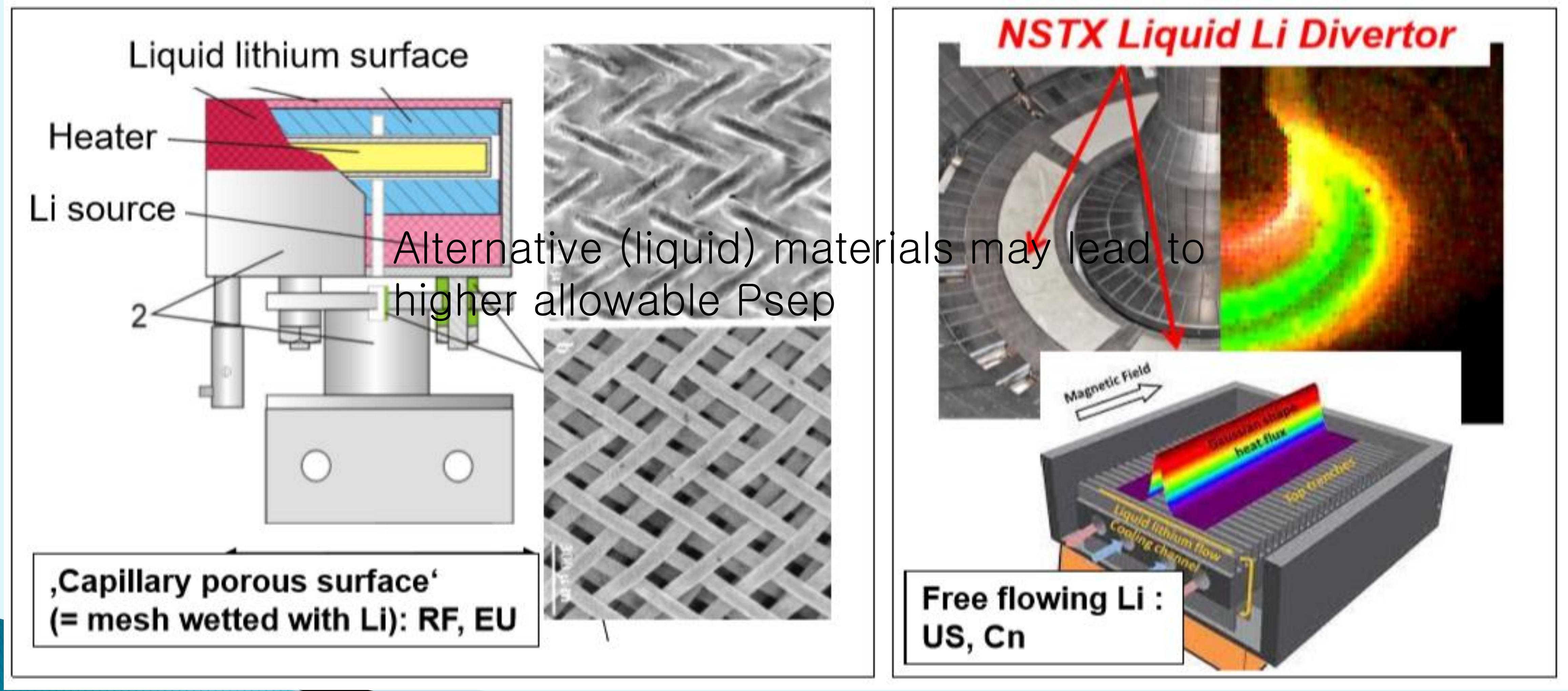

Alternative (liquid) materials may lead to higher allowable Psep

Zohm, H., *Physics of divertor power exhaust beyond ITER*, 10th ITER international school 2019.

Erosion of Plasma Facing Component (PFC)

PFC sputtering and chemical erosion

Physical sputtering yield…

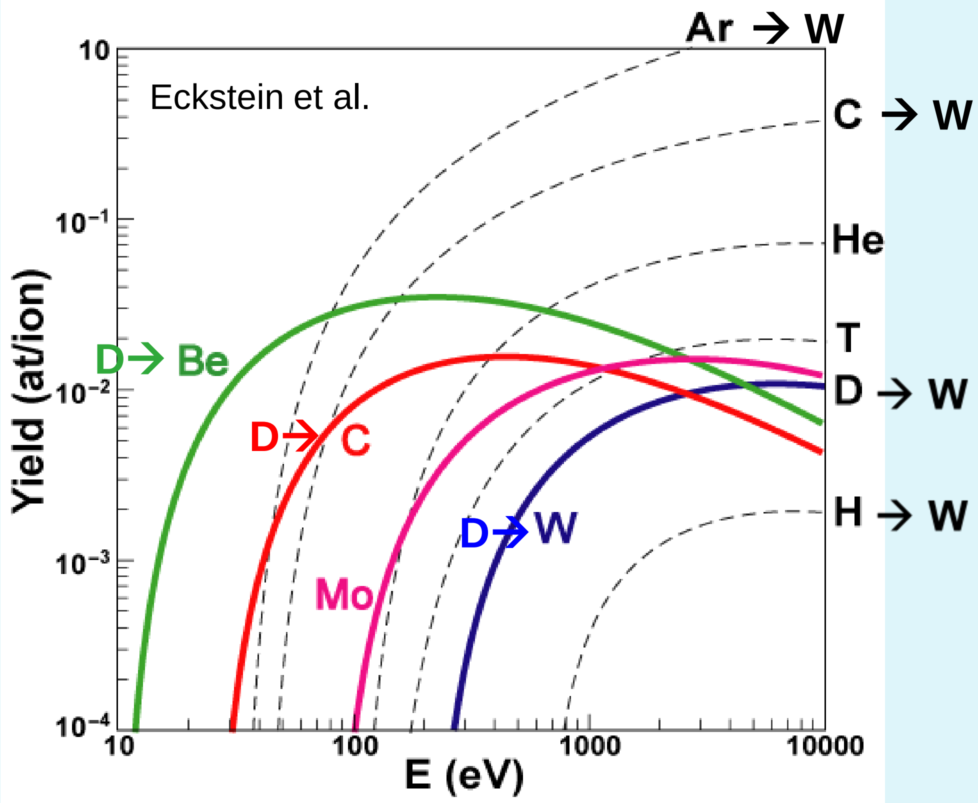

Increases with projectile energy and mass, while decreasing with target (PFC) material atomic mass

Chemical erosion yield (D on C)…

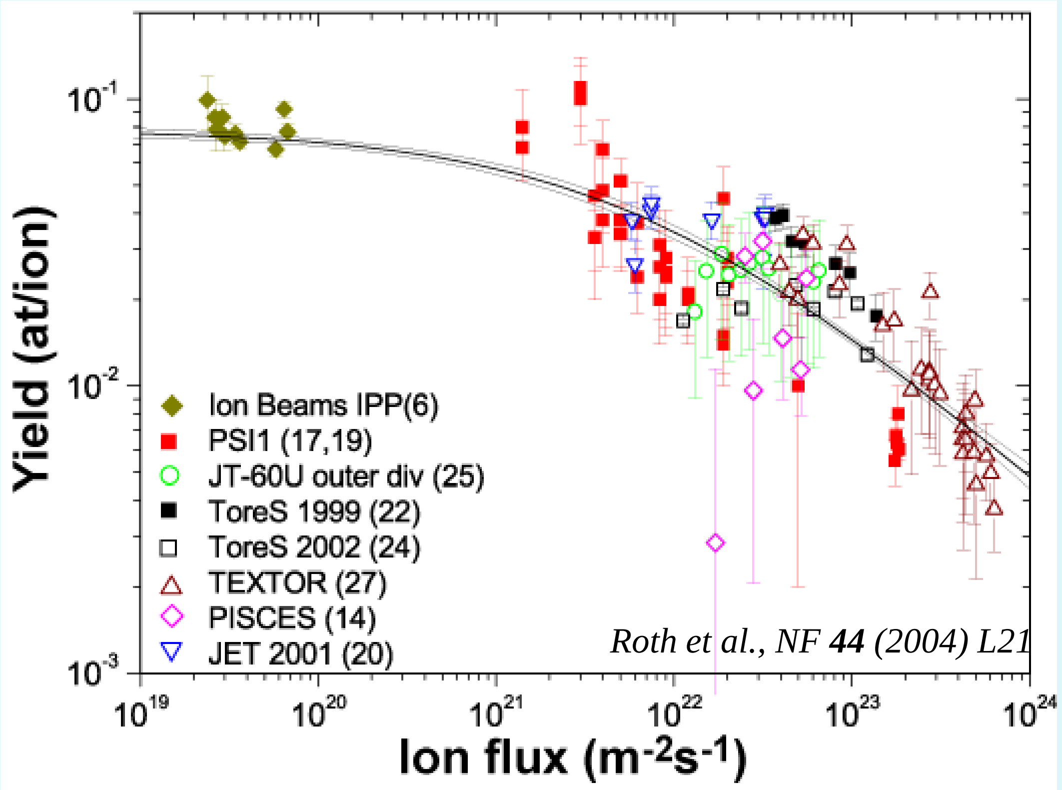

Decreases with D ion flux and is sensitive to C target temperature

Impurity Influx from Plasma Facing Component (PFC)

Impurity radiation in the core plasma

Q=(fusion power)/(power in); goal for ITER > 10

- Allowed concentration (n_W/n_e) of ~ $5x10^{-5}$
- An injection of a mm diameter droplet of W would lead to radiative collapse in ITER
- **Melting should be avoided ☺**

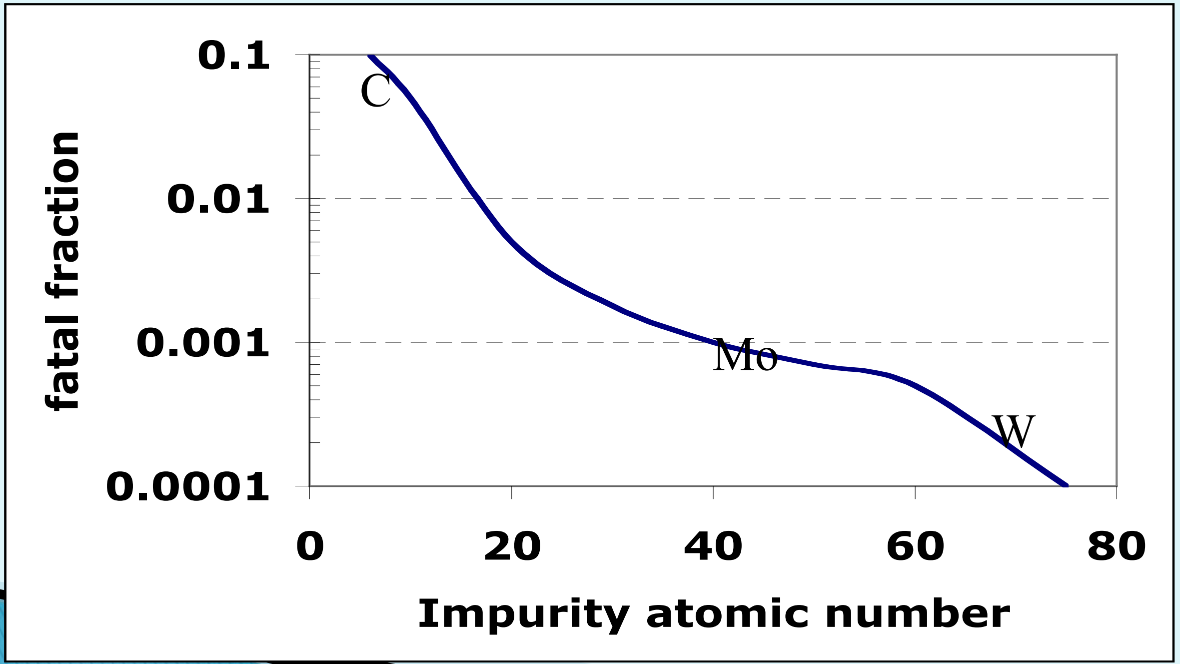

D. Whyte, 2005

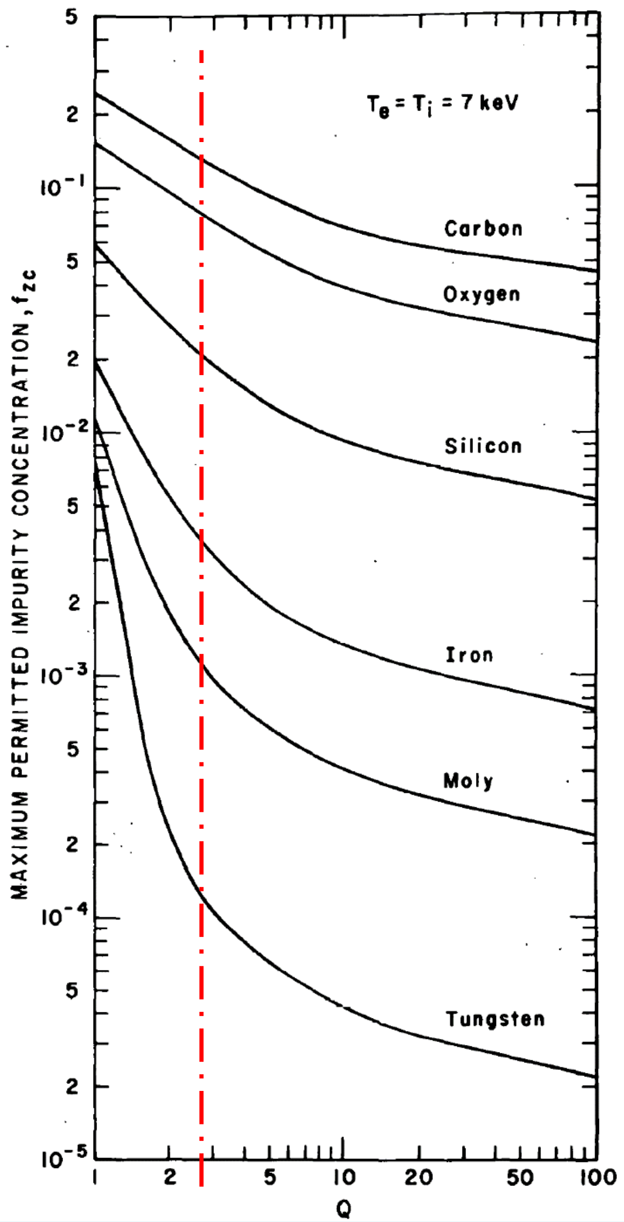

Jensen PPPL report #1350, 1977

Neutron Irradiation on Plasma Facing Component (PFC)

- Tungsten and some 3D graphites have better nuclear damage properties
- Operation at high temperature may cause 'mending' of neutron damage

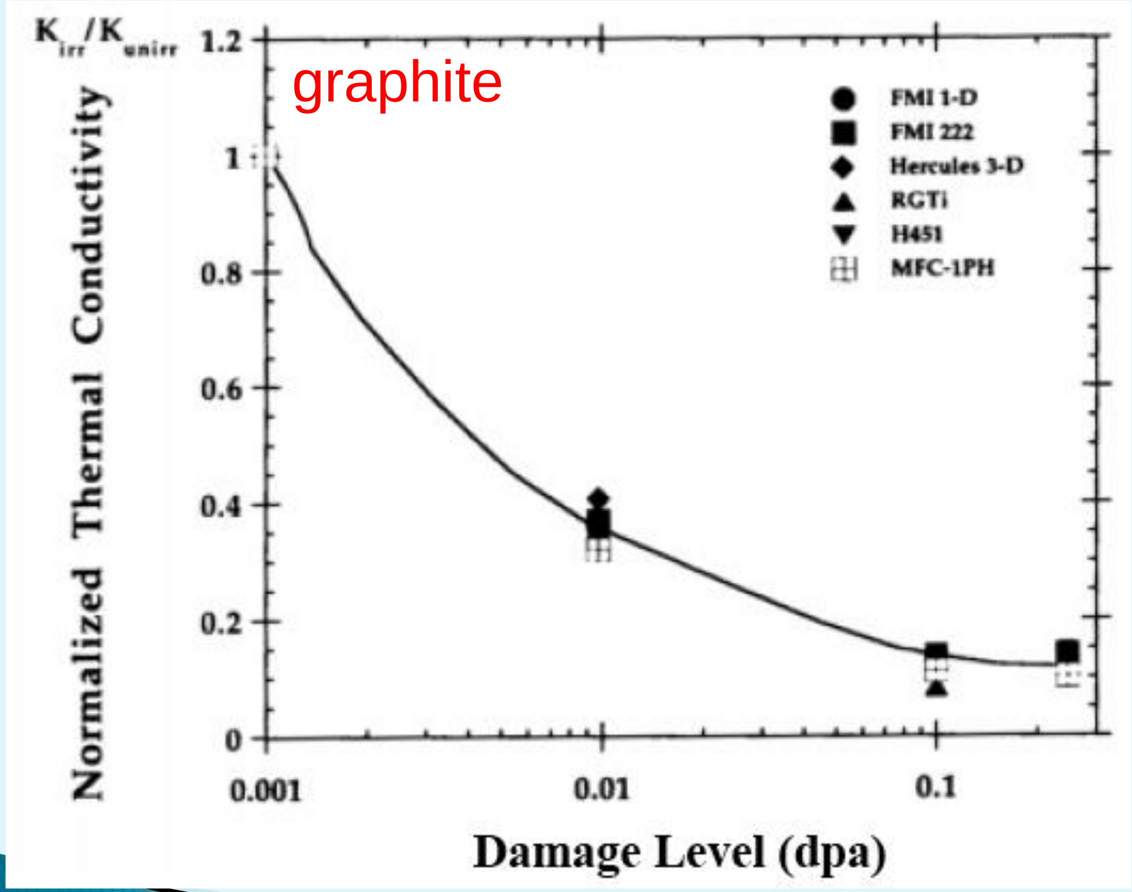

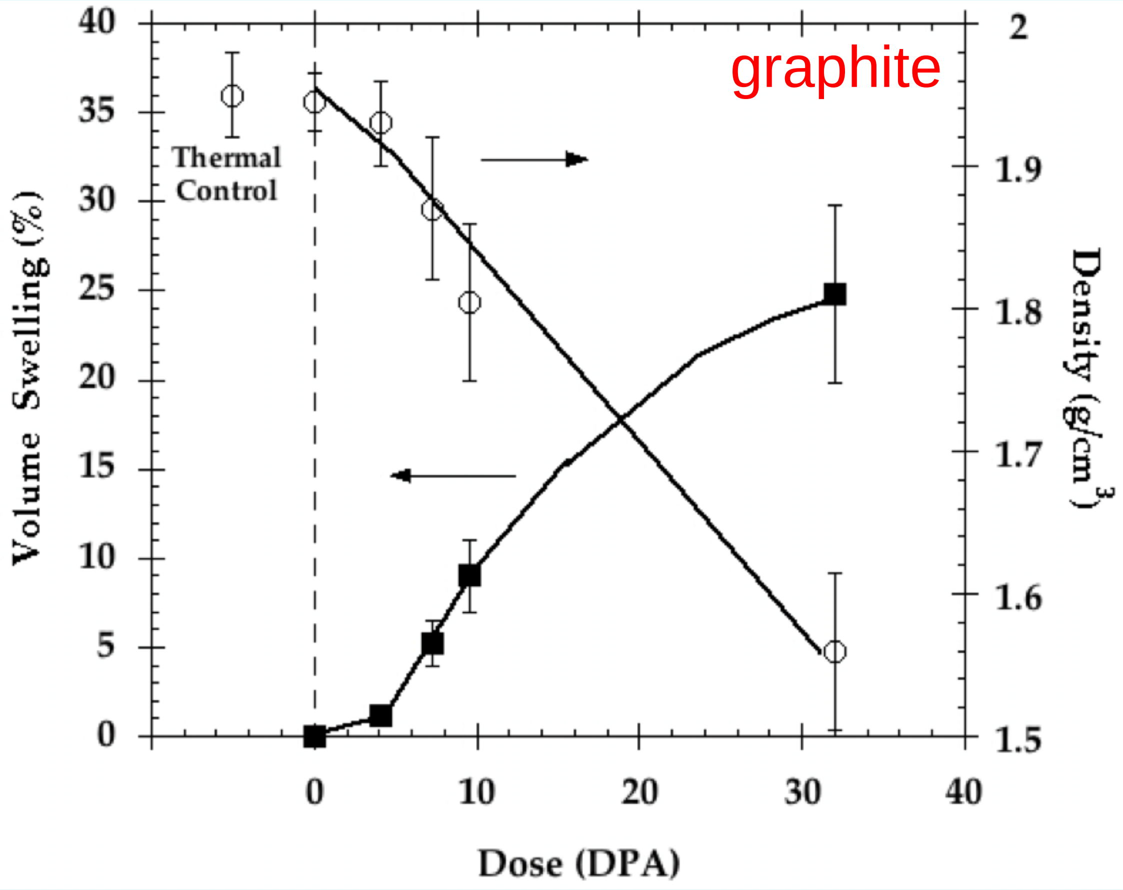

L. Snead, J of Nucl. Materials **417** (2011) 629–632

Tritium Retention of Plasma Facing Component (PFC)

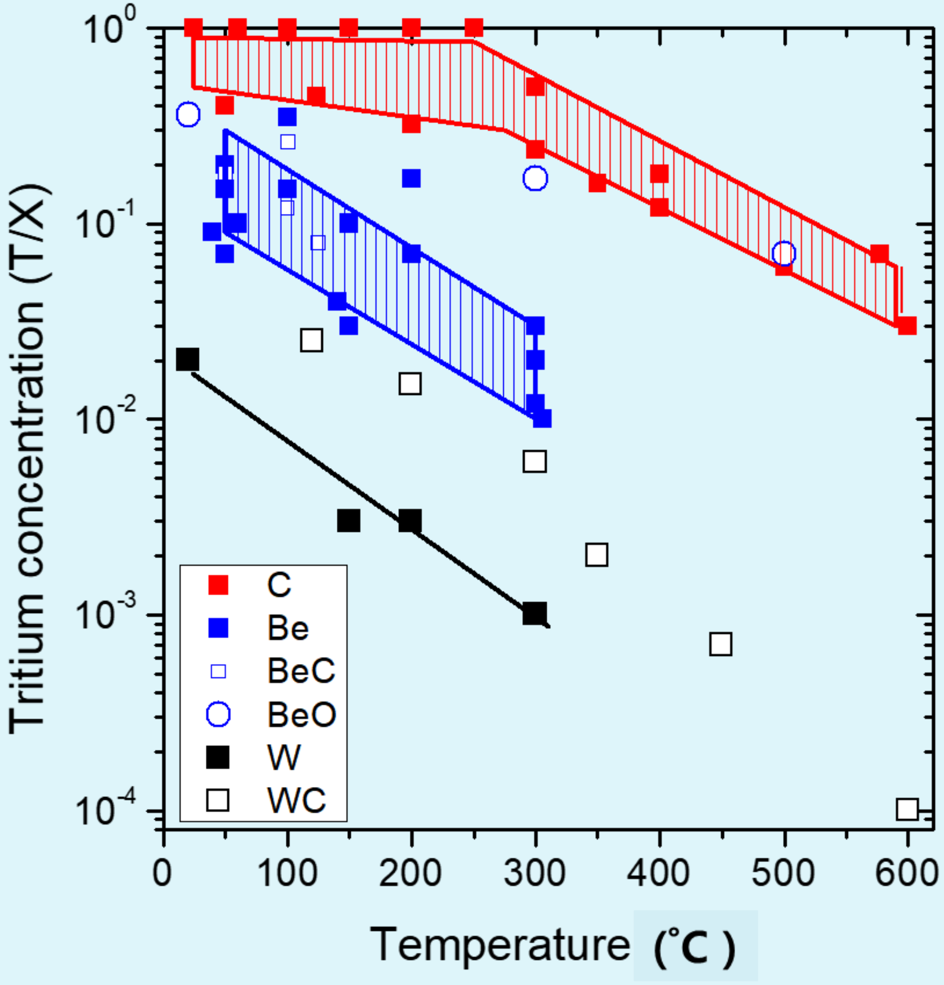

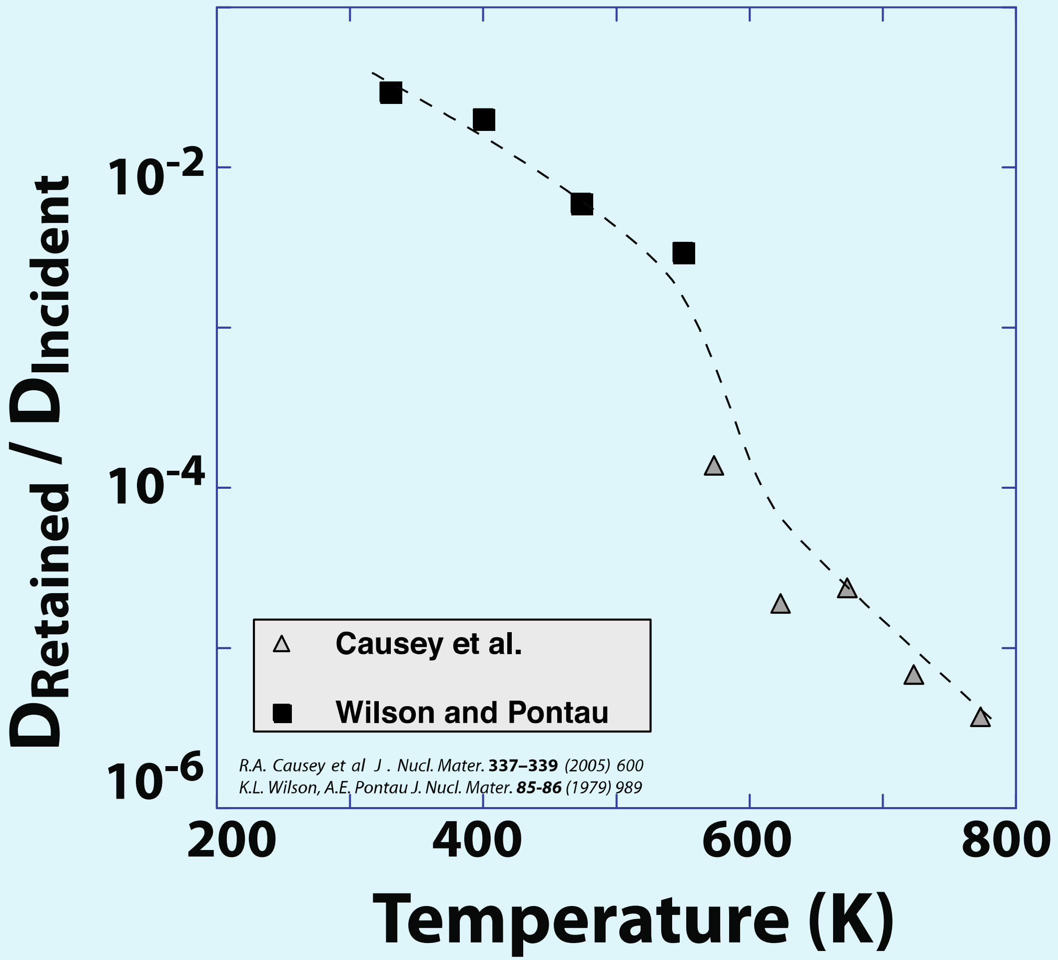

- **Implantation is the dominant retention process for refractory metals such as W**
- **Radiation Damage Increases T Retention**
- **Operating at higher temperatures lowers the retention further**

Dilution and Radiation for Fusion Operational Space

- Both dilution and radiation can be taken into account in determining the size of operational space for fusion burn through the **“Lawson criterion” (burn criterion)**

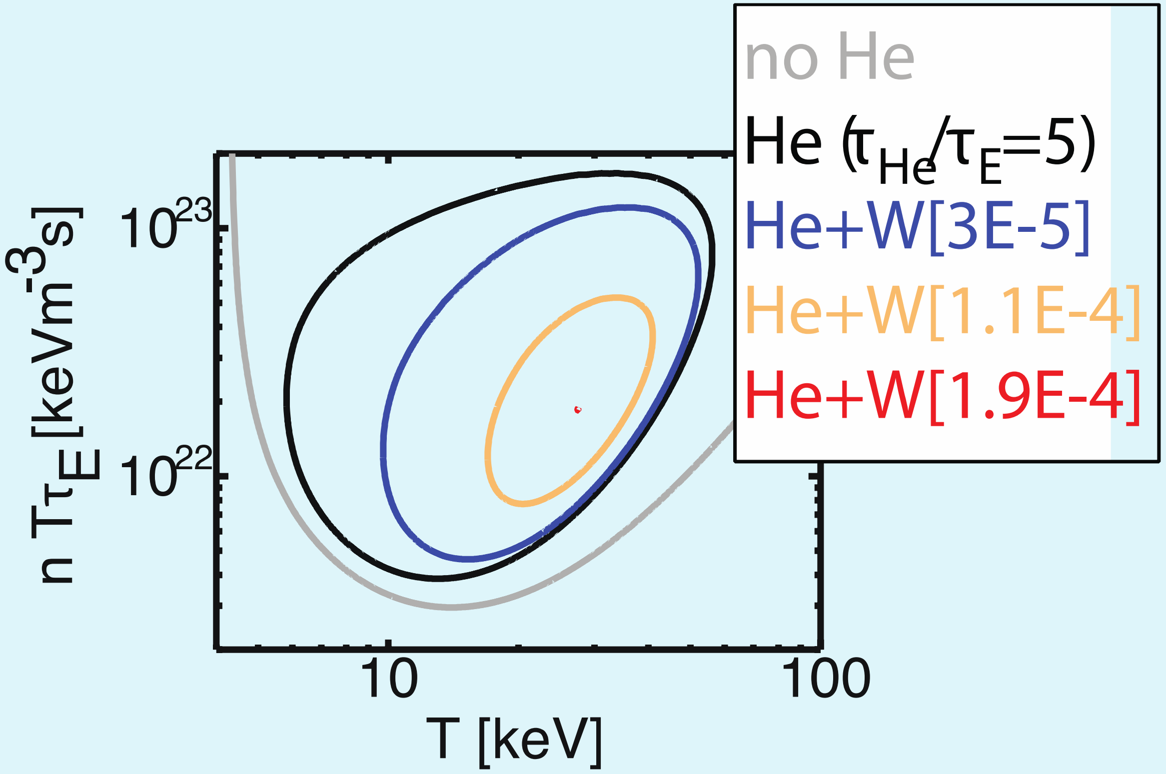

- Higher $nT\tau_E$ and higher T are needed as the He and other impurity concentrations increase.

D. Reiter et al., Nucl. Fus. 30 (1990) 2141;
T. Pütterich, EFPW Split, Dec 2014 p12

Plasma Facing Component (PFC) Material Selection

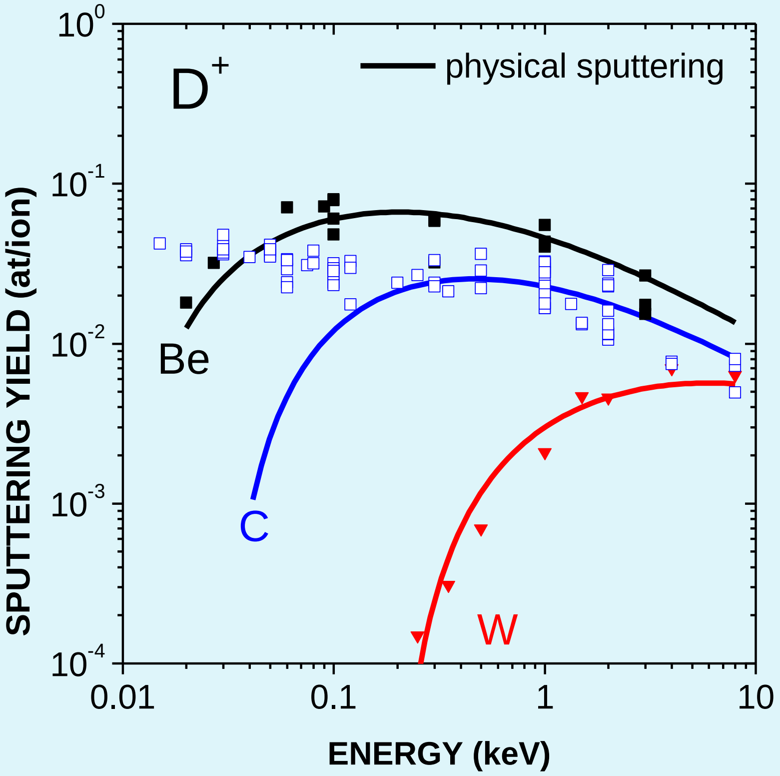

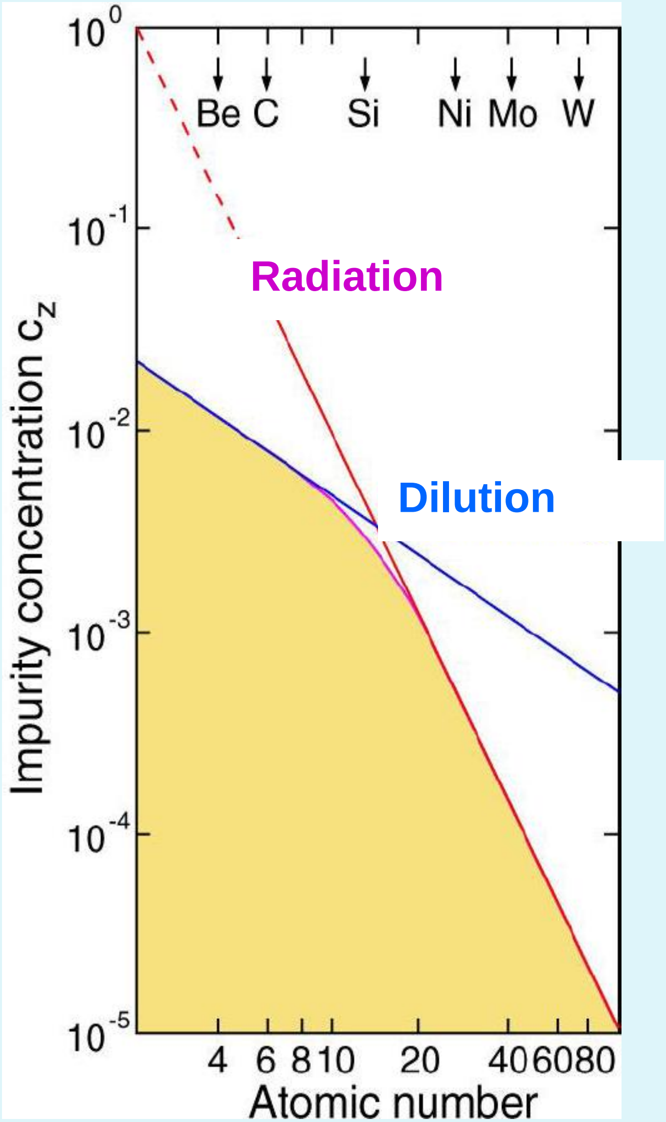

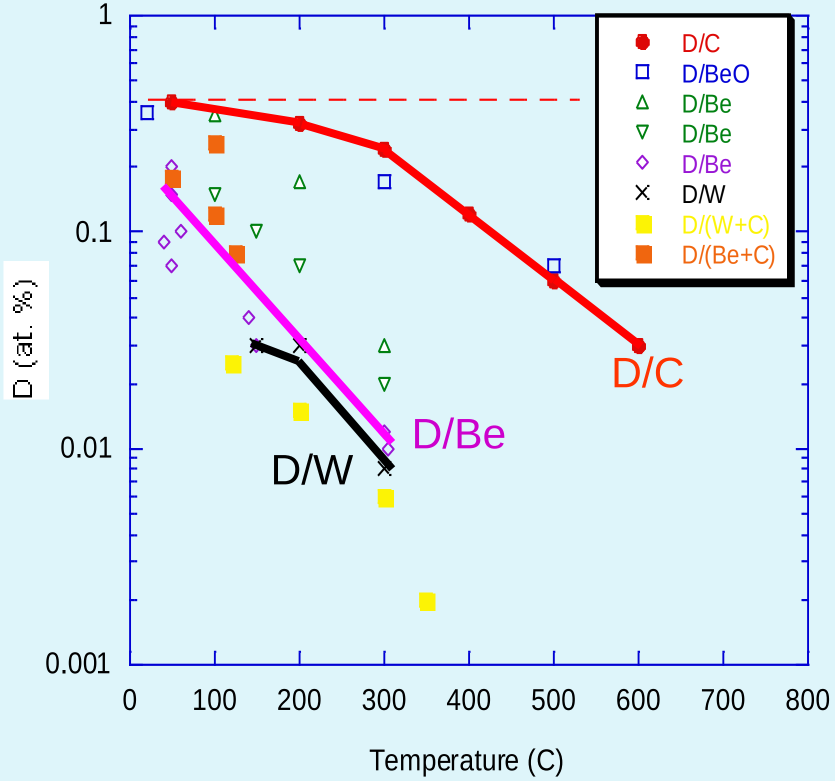

Wall erosion best with high Z
(but no melting of carbon!)

Tritium retention -
an issue for carbon!

Can fusion power be handled by surrounding wall?

Plasma Facing Component (PFC) Material selection

- High power fluxes: steady-state and transient
- Strong erosion: sputtering and chemical erosion
  - → Carbon and Beryllium unusable in reactor
  - → High-Z tungsten PFC needs improvement
- Severe neutron irradiation
- Tritium retention
  - → Carbon unusable in reactor

Tungsten

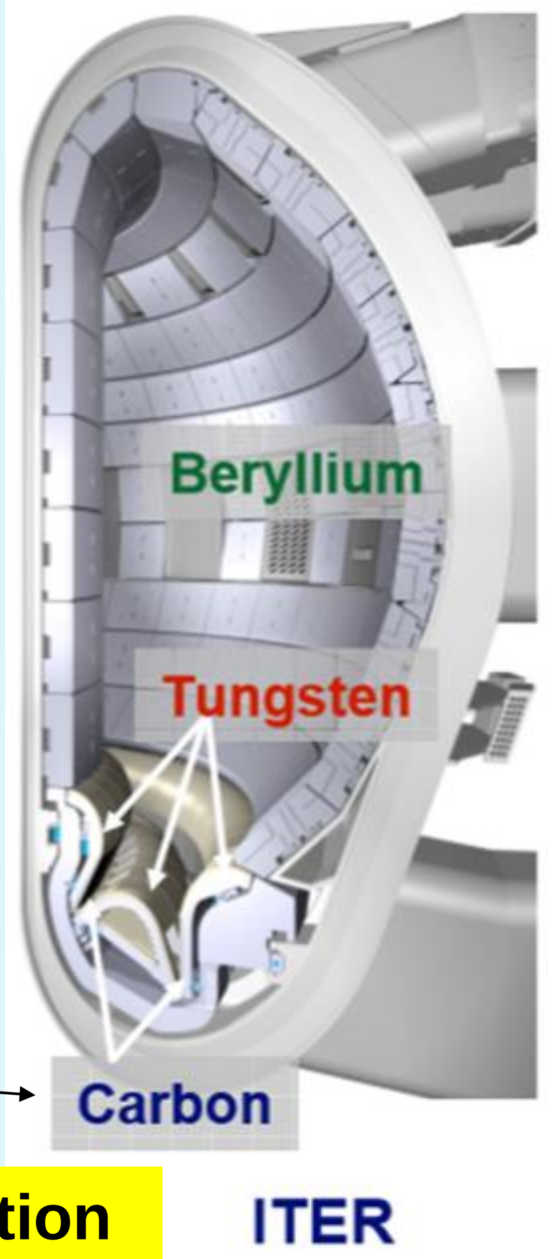

Operating at higher temperatures may be a good solution

Fusion Reactor Tech 2
14 Oct 2019

Chapt. 7 Control Systems

I. Impurities
II. Fueling
III. Impurity Control Techniques (e.g. Divertors, neutral gas blankets, etc.)

I. Impurities

Recall from ch. 3 (Vol. I) the Bremsstrahlung radiation, P_B,

$$\boxed{P_B = 5\times10^{-37}\, Z_{eff}\cdot n_e^2\, T_e^{1/2}} \quad \text{(with } T_e \text{ is in keV)} \cdots (3F14)$$

$$\text{where } Z_{eff} = \frac{\sum_k n_k \langle Z^2\rangle_k}{\underbrace{\sum_k n_k \langle Z\rangle_k}_{\equiv n_e}} = \frac{\sum_k n_k \langle Z^2\rangle_k}{n_e}, \quad \cdots (3F13)$$

which implies that, from Example Problem 4B.2 on P.78 <ch.4, Dolan, FR>, an iron ($Z=26$) fraction over 1.6 % will prevent plasma ignition at any temperature due to high Bremsstrahlung radiation loss!

- Hence, high-Z impurities (e.g., W with $Z=74$) can not be tolerated even a small density fractions ($\lesssim 10^{-4}$).
  → "line radiation" from free-bound transition reduces plasma temperature;
  → "Brem-radiation" from completely stripped impurities will also reduce plasma temperature.
- However, some line radiation from impurities which reduce "edge" plasma temperature can be beneficial since "cooler" edge plasma may produce less wall erosion and impurity flux. – Tradeoff !

$f_{zc} = \frac{n_z}{n_i}$

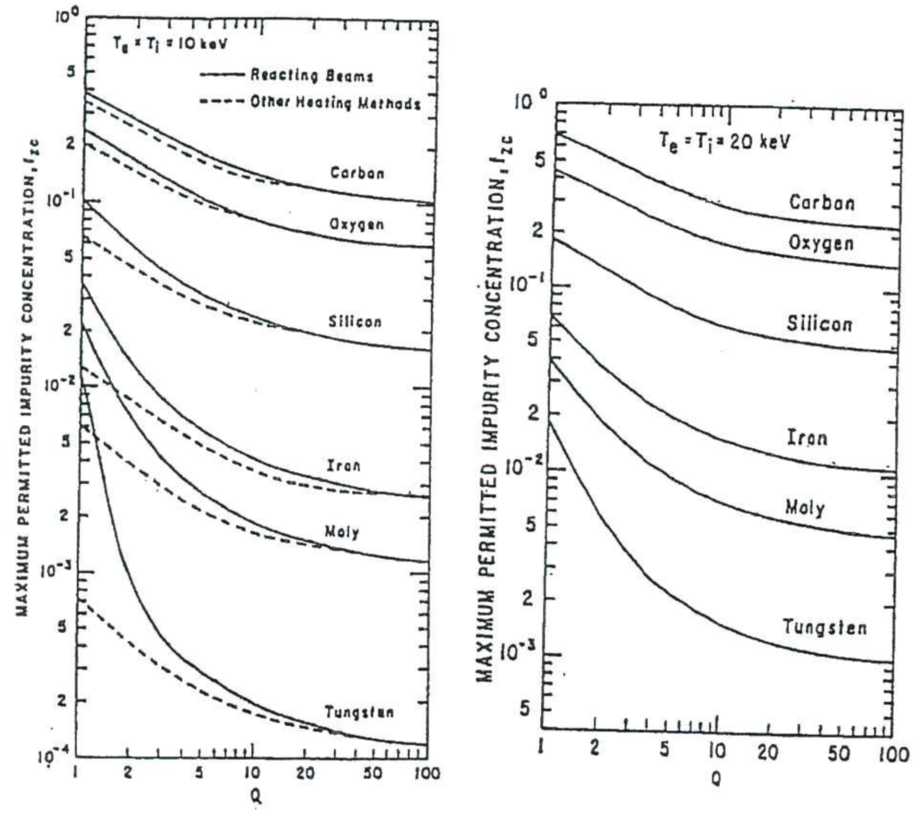

Fig. 7.1. Maximum allowed concentrations of various impurity species for attaining given Q values in a D-T plasma, using 200 keV deuteron beam heating. The dashed curves are for other heating methods, such as rf heating. From R. V. Jensen, D. E. Post, and D. L. Jassby, "Critical impurity concentrations for power multiplication in beam-heated toroidal fusion reactors", Nuclear Science and Engineering 65, 282 (1978), Figs. 3, 4. Published by ANS.

< Maximum allowable impurity concentration as function of energy multiplication, Q >

Note: As plasma temperature, T_e or T_i ↑, impurity concentration fraction could also ↑ since increased radiation cooling could be allowed for <u>high</u>-temperature background plasma.

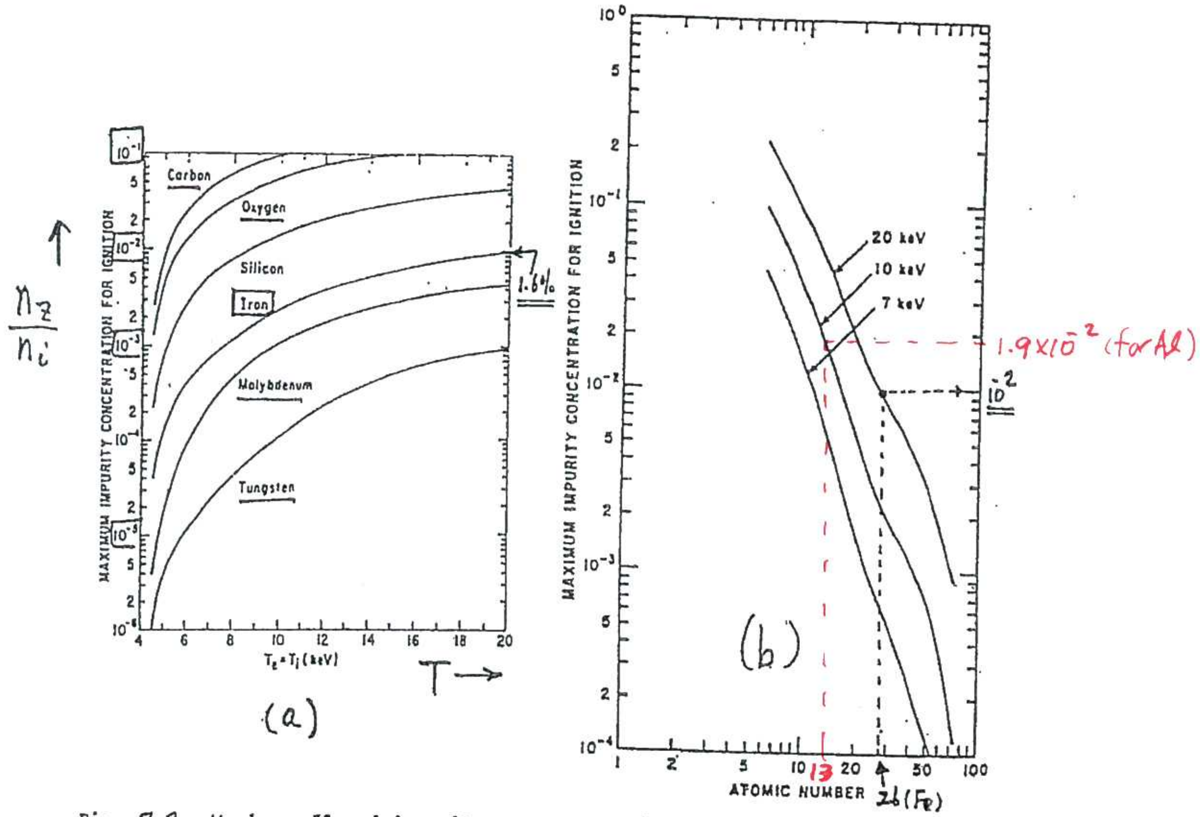

Fig. 7.2 Maximum allowed impurity concentration for ignition of a D-T plasma vs. temperature for various impurity species, and vs. atomic number for various temperatures, assuming zero nonradiative energy losses. From R. V. Jensen, D. E. Post, and D. L. Jassby, Nuclear Science and Engineering 65, 282 (1978), Figs. 5, 6. Published by ANS.

< Maximum allowed impurity concentration for ignition of D-T plasma as function of plasma temperature and of atomic number. >

Note: At 1.6 % of Iron impurity, the plasma will never ignite at any temperature from (a).

Note: as plasma temp. ↑, impurity concentration could ↑ as was illustrated from earlier Figs. 7.1 and 7.2(b). For example, iron with atomic number, Z=26 at 20 keV of plasma temperature, will be limited with the maximum allowable impurity concentration of about 10^{-2} (or ~1%).

⟹ ∴ Keep the impurity level below
- 10^{-2} for low-Z elements (O, C, N)
- 10^{-3} for intermed.-Z " (V, Fe)
- 10^{-5} for hi-Z elements (Mo, W)

7.1.2 Estimate of Equilibrium concentration of single-species impurity

Consider an impurity sputtered from the walls in a steady-state reactor:

Particle conservation eqn. for an impurity (with density n_z) is

$$V\left(\frac{dn_z}{dt}\right) = (\text{production rate by sputtering}) - (\text{net flow rate to walls})$$

$$= \left(\frac{n_i V S_i}{\tau_i} + \frac{n_\alpha V S_\alpha}{\tau_\alpha} + \frac{n_z V S_z}{\tau_z}\right) - \left(\frac{n_z V (1-R_z)}{\tau_z}\right); \quad \cdots (7.1)$$

where V = plasma volume (m^3)
n = vol. averaged density
τ = " " confinement time
S = sputtering yield
R_z = reflection coeff. for impurity w/ charge Z

subs:
- i = fuel ion
- α = alpha particle
- z = impurity species

At equilibrium, $\frac{dn_z}{dt} = 0$;

hence, $\frac{n_z}{\tau_z}\left[S_z - (1-R_z)\right] = -(n_i)\left[\frac{S_i}{\tau_i} + \frac{n_\alpha}{n_i}\frac{S_\alpha}{\tau_\alpha}\right]$

$$\Rightarrow \boxed{\frac{n_z}{n_i} = \frac{\tau_z\left(\frac{S_i}{\tau_i} + \frac{n_\alpha}{n_i}\frac{S_\alpha}{\tau_\alpha}\right)}{1 - S_z - R_z}} \quad \cdots (7.2)$$

For plasma pressure, $p = \beta \cdot B^2/2\mu_0$ and assume p = const. (for simplicity)
also let $T_e = T_i = T_\alpha = T_z = T$.

$$\rightarrow \boxed{(n_e + n_i + n_\alpha + n_z)\,kT} = p = \text{const} \equiv \boxed{2 n_0 kT}, \quad \cdots (7.3)$$

(where $n_i = n_e = n_0$ when $n_\alpha = n_z = 0$)

By quasineutrality, $\boxed{n_e = n_i + 2n_\alpha + z n_z}$ (z = impurity charge number) $\cdots (7.4)$

Example 7.1

Estimate "Be" impurity fraction and the reduction of D-T fusion power density for the case of steady-state reactor with walls coated with "Be" under the following plasma conditions:

$T_{\substack{edge\\plasma}} = 200\ eV$, impurity reflect$^{=}$ coeff. $R_Z = 0.05$, $\frac{n_\alpha}{n_i} = 10^{-1}$,

and $\tau_Z = \tau_\alpha = \tau_i$.

Ans.

Note: Table 8.8 → sputtering yields

Table 24G2. Predicted sputtering yields for Maxwellian ions on various materials. S_z represents self-sputtering. Subscripts 1 and 2 represent the two elements of a compound, in order. For BeO, S_{z1} represents sputtering by Be and S_{z2}, by O. From D. L. Smith, Journal of Nuclear Materials 75, 20-31 (1978), Table 4. Research performed at ANL.

Material	T_I (eV)	S_D	S_T	S_{He}	S_{z1}	S_{z2}
Be	60	0.0187	0.0280	0.0546	0.1571	
	200	0.0224	0.0337	0.0858	0.3142	
	1000	0.0140	0.0210	0.0742	0.3899	
B	60	0.0105	0.0160	0.0297	0.1040	
	200	0.0140	0.0210	0.0508	0.2365	
	1000	0.0096	0.0145	0.0492	0.3716	
C	60	0.0081	0.0121	0.0220	0.0851	

$S_i\Big|_{200\,eV} = (\overbrace{D\ and\ T}^{average}) = \frac{0.0224 + 0.0337}{2} = 0.02805$

$S_\alpha\Big|_{200\,eV} = 0.0858$

$S_Z\Big|_{200\,eV} = 0.3142$ (by Be, not by O) $(Z = Be)$

$\therefore$ Eq. (7.2) → $\boxed{\frac{n_Z}{n_i}} = \frac{\tau_Z\left(\frac{S_i}{\tau_i} + \frac{n_\alpha}{n_i}\frac{S_\alpha}{\tau_\alpha}\right)}{1 - S_Z - R_Z} = \frac{0.0281 + (0.1)\,0.0858}{1 - 0.3142 - 0.05}$

↑ impurity fraction

$= \boxed{0.05769}$

For Be$\Big|_{Z=4}$, this is well below max. concentration for ignition (cf. Fig. 7.2(a)) for Z = 4.

To find the reduction of D-T fusion power density:

Quasineutrality → $n_e = n_i + 2n_\alpha + 4n_Z$

$= n_i\left[1 + 2(0.1) + 4(0.058)\right] = 1.432\,n_i$

Since $(n_i + n_e + n_\alpha + n_Z)kT = p_0 = 2n_0 kT$,

$n_i(1 + 1.432 + 0.1 + 0.058) = 2n_0 \Rightarrow \frac{n_i}{n_0} = \frac{2}{2.59} = 0.772$

Recall also that $\frac{P_f}{P_0} = \left(\frac{n_i}{n_0}\right)^2 = \boxed{0.5962}$ (since $P_f \propto n_i^2 \langle\sigma v\rangle W_{fusion}$)

Thus, the fusion power density is reduced to 60% of its original power because of Be-impurity (with 5.769%).

Prob. 7.1 Let's find out the maximum impurity concentration that prevents ignition. Consider a steady-state reactor with aluminum walls with $n_\alpha/n_i = 12\%$, plasma edge temperature = 60 eV, and $R_Z = 0.2$ (impurity reflection coefficient) for aluminum. Assume equal particle confinement times for all species. Estimate the equilibrium fraction of aluminum in the plasma, the reduction of fusion power density by the helium and aluminum, and whether ignition would be prevented by this aluminum concentration at 10 keV DT plasma.

— ◡ —

The equilibrium fractional concentration of aluminum is for $n_Z = n_{Al}$

$$\frac{n_Z}{n_i} = \frac{\tau_Z\left(S_i/\tau_i + n_\alpha S_\alpha/n_i\tau_\alpha\right)}{1 - S_Z - R_Z}\Bigg|_{\tau_i=\tau_Z=\tau_\alpha} = \frac{S_i + S_\alpha \cdot n_\alpha/n_i}{1 - S_Z - R_Z} = \frac{\frac{1}{2}(0.0108+0.0164)+(0.0260\cdot 0.12)}{1-0.2088-0.2}$$

$$= \boxed{0.028} \Leftarrow n_{Al}/n_i$$

Table 8.8 Predicted sputtering yields for Maxwellian ions on various materials

	T_i (eV)	S_D	S_T	S_{He}	S_{z1}	S_{z2}
Be	60	0.0187	0.0280	0.0546	0.1571	
	200	0.0224	0.0337	0.0858	0.3142	
	1000	0.0140	0.0210	0.0742	0.3899	
B	60	0.0105	0.0160	0.0297	0.1040	
	200	0.0140	0.0210	0.0508	0.2365	
	1000	0.0096	0.0145	0.0492	0.3716	
C	60	0.0081	0.0121	0.0220	0.0851	
	200	0.0115	0.0173	0.0401	0.2113	
	1000	0.0086	0.0130	0.0427	0.3999	
Al	60	0.0108	0.0164	0.0260	0.2088	
	200	0.0204	0.0307	0.0598	0.6383	
	1000	0.0227	0.0341	0.0959	2.221	

The reduction in fusion power density,

$$\frac{P_f}{P_{f0}} = \left(\frac{n_i}{n_0}\right)^2, \quad \text{note: } n_i + 2n_\alpha + 13n_{Al} = n_e$$

$$\rightarrow n_e = 1.604\, n_i$$

Also, $(n_e + n_i + n_\alpha + n_Z)kT = 2n_0 kT$

$$\rightarrow \frac{n_i}{n_0} = 2\left(\frac{n_e}{n_i} + 1 + \frac{n_\alpha}{n_i} + \frac{n_Z}{n_i}\right)^{-1}$$

$$\therefore \frac{P_f}{P_{f0}} = 4(1.604 + 1 + 0.12 + 0.028)^{-2} = \boxed{0.528}$$

Reduction of 47.2 %

Maximum impurity concentration for ignition vs. atomic number (cf. Fig. 7.2(b)) at Z=13, T=10 keV is $(n_Z/n_i)_{max} \simeq 1.9\times10^{-2}$; since $\frac{n_Z}{n_i} = 2.8\times10^{-2} > 1.9\times10^{-2}$, No ignition.

7.1.3 Helium accumulation and its equilibrium concentration

$$D + T \rightarrow n + {}^4He$$ ← helium "ash" after thermalization

(50/50 DT)

α-pcle conservation eqn.:

$$\frac{dn_\alpha}{dt} = \frac{1}{4} n_i^2 \langle\sigma v\rangle_{DT} - \frac{n_\alpha(1-R_\alpha)}{\tau_\alpha} \quad \cdots (7.5)$$

[τ_α = α-pcle conf. time]

$\frac{1}{4} n_i^2 \langle\sigma v\rangle_{DT}$: α-pcle production rate

Here, $\frac{n_\alpha}{\tau_\alpha}(1-R_\alpha)$: net flow rate to walls (if a fraction R_α of α-pcles incident on the walls is reflected back into the plasma)

Assume $n_z = 0$ (no impurity other than α-pcle) for simplicity.

Let $f_\alpha \equiv \frac{n_\alpha}{n_0}$.

Recall: $(n_e + n_i + n_\alpha + \cancel{n_z}^{\,0})kT \equiv 2n_0 kT$ & $(n_i + 2n_\alpha + \cancel{Zn_z}^{\,0}) = n_e$ $\rightarrow n_i = n_0 - \frac{3n_\alpha}{2} = n_0\left(1 - \frac{3}{2}f_\alpha\right) \cdots (7.6)$

If no α-pcle is removed thru the wall, i.e., if $R_\alpha = 1$ (α-pcles all reflected),

$$\left[\frac{dn_\alpha}{dt} = \frac{1}{4} n_i^2 \langle\sigma v\rangle_{DT}\right] \times\frac{1}{n_0} \rightarrow \frac{df_\alpha}{dt} = \frac{1}{4}\langle\sigma v\rangle_{DT} \cdot \frac{n_i^2}{n_0} \times \left(\frac{n_0}{n_0}\right)$$

$$= \frac{1}{4}\langle\sigma v\rangle_{DT}\, n_0 \cdot \left(\frac{n_i}{n_0}\right)^2 = A_1\left(1 - \frac{3}{2}f_\alpha\right)^2$$

where $\frac{1}{4}\langle\sigma v\rangle_{DT}\, n_0 \equiv A_1$ and $\left(\frac{n_i}{n_0}\right)^2 \equiv \left(1 - \frac{3}{2}f_\alpha\right)^2$

If $f_\alpha(t)\big|_{t=0} = 0$,

$$f_\alpha(t) = \frac{A_1 t}{1 + 3A_1 t/2}$$

∴ The reduction in fusion power due to α-pcle accumulation is

$$\frac{P_f(t)}{P_{f0}} = \left(\frac{n_i}{n_0}\right)^2 = \left(1 - \frac{3}{2}f_\alpha\right)^2 = \left(1 + \frac{3}{2}A_1 t\right)^{-2} \quad \cdots (7.8)$$

Example 7.2

Estimate the time that takes for the helium accumulation to reduce the fusion power density by a factor of two if the helium ash is not removed from the reactor with $n_0 = 10^{20}\ m^{-3}$ and $T = 20$ keV.

ans. From eq. (7.8),

$$\frac{P_f(t)}{P_{f0}} = \left(\frac{n_i}{n_0}\right)^2 = \left(1 + \frac{3}{2} A_1 t\right)^{-2},$$

where $\left(\frac{n_i}{n_0}\right)^2 = \left(1 - \frac{3}{2} f_\alpha\right)^2$,

one solves it for time t to find

$$t = \left[\left(\frac{P_{f0}}{P_f(t)}\right)^{1/2} - 1\right] \Big/ \frac{3}{2} A_1$$

Recall, $A_1 = \frac{1}{4} \langle \sigma v \rangle_{DT}\, n_0$ (at $T = 20$ keV)

$= \frac{1}{4} \cdot \left(0.424 \times 10^{-21}\ \frac{m^3}{sec}\right) \cdot 10^{20}\ m^{-3}$ (from Table 2C1, p. 28, Vol. I, FR)

$= 0.0106\ sec^{-1}$,

and $\frac{P_{f0}}{P_f(t)} = \frac{1}{\left(\frac{1}{2}\right)} = 2$ (Given as a condition in the problem).

Hence, $t = \left[\sqrt{2} - 1\right] \Big/ \left(\frac{3}{2} \times 0.0106\right)$

$= \underline{26.05\ sec}$

If α-ptcles are not removed from the reactor, the original fusion power will be reduced to half within 26.05 sec

Note:
- $t \lesssim 30$ sec → short pulse mode (fusion burn occurs until impurity quenches it.)
- $t \gtrsim 30$ sec → long pulse mode (impurity control & refueling)
- steady-state operation → very effective impurity control and reduction

More general solution of Eq. (7.5):

i.e.,
$$\boxed{\frac{dn_\alpha}{dt} = \frac{1}{4} n_i^2 \langle\sigma v\rangle_{DT} - \frac{n_\alpha}{\tau_\alpha}(1-R_\alpha)} \cdots (7.5)$$

Consider $R_\alpha \approx 1$ but $\boxed{R_\alpha < 1}$

Recall, eq. (7.6), $n_i = n_0(1 - \frac{3}{2} f_\alpha)$ [with $f_\alpha \equiv \frac{n_\alpha}{n_0}$] ($n_0$: const.)

Note: $n_\alpha = n_0 f_\alpha$

$$\therefore \frac{d(n_0 f_\alpha)}{dt} = \frac{\langle\sigma v\rangle_{DT}}{4}\left[n_0(1-\frac{3}{2}f_\alpha)\right]^2 - \frac{n_0 f_\alpha}{\tau_\alpha}(1-R_\alpha)$$

Since n_0 = const,

$$\boxed{\frac{df_\alpha}{dt} = \frac{\langle\sigma v\rangle_{DT}}{4 n_0} n_0^2 \left[1-\frac{3}{2}f_\alpha\right]^2 - \frac{n_0 f_\alpha(1-R_\alpha)}{n_0 \cdot \tau_\alpha}}.$$

[Let $\theta \equiv (1-R_\alpha)\frac{t}{\tau_\alpha}$, and $A \equiv n_0 \langle\sigma v\rangle_{DT} \tau_\alpha / 4(1-R_\alpha)$.

then $\frac{d\theta}{dt} = (1-R_\alpha)\frac{1}{\tau_\alpha}$.]

$$\left(\frac{df_\alpha}{dt}\right)\cdot\left(\frac{\tau_\alpha}{1-R_\alpha}\right) = \frac{\langle\sigma v\rangle_{DT}}{4} n_0 (1-\frac{3}{2}f_\alpha)^2 \left(\frac{\tau_\alpha}{1-R_\alpha}\right) - \frac{f_\alpha(1-R_\alpha)}{\tau_\alpha}\cdot\left(\frac{\tau_\alpha}{1-R_\alpha}\right)$$

where $\frac{\tau_\alpha}{1-R_\alpha} = \frac{1}{(d\theta/dt)}$ and $\frac{\langle\sigma v\rangle_{DT}}{4} n_0 \frac{\tau_\alpha}{1-R_\alpha} \equiv A$

$$\Rightarrow \boxed{\left(\frac{df_\alpha}{d\theta}\right) = A(1-\frac{3}{2}f_\alpha)^2 - f_\alpha}$$

To obtain the solution $f_\alpha(\theta)$:

$$\frac{df_\alpha}{[A(1-\frac{3}{2}f_\alpha)^2 - f_\alpha]} = d\theta,$$

$[A(1-3f_\alpha + \frac{9}{4}f_\alpha^2) - f_\alpha]$

$\Rightarrow \underbrace{A\cdot\frac{9}{4}}_{\equiv c} f_\alpha^2 \underbrace{-(3A+1)}_{\equiv b} f_\alpha + \underbrace{A}_{\equiv a}$

Let $X = a + bx + cx^2$ $[x \equiv f_\alpha]$

and $q = 4ac - b^2$

then, $q = 4 \cdot A \cdot (\frac{9}{4}A) - (-3A-1)^2$

$= 9A^2 - (9A^2 + 6A + 1) = -6A - 1 \qquad \therefore \underline{q < 0}$

Now, $\displaystyle\int_{f_\alpha=0}^{f_\alpha(\theta)} \frac{df_\alpha}{[A(1-\frac{3}{2}f_\alpha)^2 - f_\alpha]^2} = \int_{\theta=0}^{\theta} d\theta = \theta$

$\Downarrow$

$$\int \frac{dx}{X} = \frac{-2}{\sqrt{-q}} \tanh^{-1} \frac{2cx+b}{\sqrt{-q}} \qquad (q<0)$$

at $\theta=0$, $f_\alpha(0) = 0$ (given condition) $\Rightarrow$ $x = f_\alpha = 0$

at $\theta=\theta$, $f_\alpha(\theta)$ $\Longrightarrow$ $x = f_\alpha(\theta)$

$$\therefore \int_{x=0}^{x=f_\alpha(\theta)} \frac{dx}{X} = \theta \quad \Rightarrow \left[\frac{-2}{\sqrt{-q}} \tanh^{-1} \frac{2cx+b}{\sqrt{-q}}\right]_0^x = \theta$$

$$\Rightarrow -\frac{2}{\sqrt{-q}}\left[\tanh^{-1}\frac{2cx+b}{\sqrt{-q}} - \tanh^{-1}\frac{b}{\sqrt{-q}}\right] = \theta$$

$$\Rightarrow \tanh^{-1}\frac{2cx+b}{\sqrt{-q}} = \frac{\sqrt{-q}}{-2}\theta + \tanh^{-1}\frac{b}{\sqrt{-q}}$$

$$\Rightarrow 2cx+b = \sqrt{-q}\tanh\left[\frac{\sqrt{-q}}{-2}\theta + \tanh^{-1}\frac{b}{\sqrt{-q}}\right]$$

$$\Rightarrow \underset{f_\alpha(\theta)}{x} = \frac{1}{2c}\left\{\sqrt{-q}\tanh\left[\frac{\sqrt{-q}}{-2}\theta + \tanh^{-1}\frac{b}{\sqrt{-q}}\right] - b\right\}$$

$$\therefore \boxed{f_\alpha(\theta)} = \frac{1}{2\cdot(\frac{9}{4}A)}\left\{\sqrt{6A+1}\tanh\left[\frac{\sqrt{6A+1}}{-2}\theta + \tanh^{-1}\frac{(-3A-1)}{\sqrt{6A+1}}\right] + (3A+1)\right\}$$

$$\boxed{= \frac{3A+1}{4.5A} - \frac{(6A+1)^{1/2}}{4.5A}\tanh\left[\tanh^{-1}\frac{(3A+1)}{(6A+1)^{1/2}} + \frac{(6A+1)^{1/2}\theta}{2}\right]}$$

7.1.4 Equilibrium He concentration

Assume no other impurities other than α-pcle, $\therefore n_z = 0$.
Recall the burn up fraction (f_b) for a steady-state DT reactor from eq. (407) (p. 87, vol. I of Dolan's FR)

$$f_b = \frac{n_i^2 \langle\sigma v\rangle_{DT}/2}{n_i^2\langle\sigma v\rangle_{DT}/2 + \frac{n_i}{\tau_p}} \xrightarrow[\tau_p \equiv \tau_i]{\text{For } f_b \ll 1} \boxed{f_b \simeq n_i \tau_i \langle\sigma v\rangle_{DT}/2}$$

Equilibrium solution of

$$\frac{dn_\alpha}{dt} = \frac{1}{4} n_i^2 \langle\sigma v\rangle_{DT} - \frac{n_\alpha(1-R_\alpha)}{\tau_\alpha} \xrightarrow{\text{"}\frac{dn_\alpha}{dt}=0\text{"}} \boxed{\frac{n_\alpha}{n_i} \equiv a}$$

$$= \frac{n_i\langle\sigma v\rangle_{DT}\,\tau_\alpha}{4(1-R_\alpha)}$$

$$= f_b \, \frac{1}{2\tau_i} \, \frac{\tau_\alpha}{(1-R_\alpha)} \quad \cdots (7.12)$$

Helium concentration, f_α

$$f_\alpha \equiv \frac{n_\alpha}{n_0} = \left(\frac{n_\alpha}{n_i}\right)\left(\frac{n_i}{n_0}\right)$$

where $\frac{n_\alpha}{n_i} = a$ and $\frac{n_i}{n_0} = 1 - \frac{3}{2}\frac{n_\alpha}{n_0}$.

Recall: $n_i = n_0 - \frac{3}{2} n_\alpha$ (Eq. 7.6)

$$\Rightarrow \left(\frac{n_i}{n_0}\right) = 1 - \frac{3}{2}\frac{n_\alpha}{n_0}$$

$$\frac{n_\alpha}{n_0}\left(1 + \frac{3}{2}a\right) = a$$

$$\therefore f_\alpha = \boxed{\frac{n_\alpha}{n_0} = \frac{a}{1+\frac{3}{2}a}}$$

The power reduction caused by helium alone is

$$\frac{P_f}{P_{f0}} = \left(\frac{n_i}{n_0}\right)^2 = \left(1 - \frac{3}{2} f_\alpha\right)^2 = \left(1 - \frac{3}{2}\cdot\frac{a}{(1+\frac{3}{2}a)}\right)^2 = \left(1 + \frac{3a}{2}\right)^{-2}$$

To keep $P_f/P_{f0} \geq 1/2$, one needs $\frac{1}{2} \leq \left(1+\frac{3}{2}a\right)^{-2} \Rightarrow a \leq \frac{2}{3}(\sqrt{2}-1) = \underline{0.276}$

[$P_f/P_{f0} = 1/2 \Rightarrow (n_\alpha/n_0) \simeq 0.276/(1+(\frac{3}{2}\times 0.276)) = 0.195 \Rightarrow 19.5\%$]

II. Fueling (§7.4)

i) plasma guns –

pcles > 10^{21} per shot for plasma energy of MJ range at 50% efficiency.

Fusion power,

$$P_F = f_b \, S_i \, V \cdot \frac{W_{DT}}{2}$$

- f_b: burn up fraction
- S_i: fuel ion source $\left(\frac{ions}{m^3 \cdot sec}\right)$
- V: plasma volume (m^3)
- $\frac{W_{DT}}{2}$: energy that "each" fuel produces

∴ Required fuel ion source;

$$\boxed{S_i V = \frac{2 P_F}{f_b W_{DT}}} \quad (\text{ions/sec})$$

e.g. If fusion reactor produces $P_F = 3.3$ GW (thermal) with $f_b = 0.05$ (5%),

then
$$S_i V = \frac{2 \times 3.3 \times 10^9}{0.05 \times 17.6 \times 10^6 \times 1.6 \times 10^{-19}}$$
$$= 4.68 \times 10^{22} \ (\text{ions/sec})$$

↑ required fueling rate

ii) neutral beams –

Required current for fueling

$$\boxed{I = e S_i V = \frac{2 e P_F}{f_b W_{DT}}}$$

e.g. For $P_F = 3.3$ GW, $f_b = 0.05$;

$$I = \left(4.68 \times 10^{22} \frac{ions}{sec}\right)\left(1.6 \times 10^{-19} \text{ coul}\right) = 7.5 \times 10^3 \text{ amp} = 7.5 \text{ kA}$$

iii) pellet injection (§7.4.6)

solid D or T w/ diameters of 1-10 mm.

Required velocity to penetrate a distance l into the plasma radius of a (m):

$$u = a \frac{1}{(M)^{1/3}} \frac{1}{(f V)^{5/9}} \frac{1}{\langle n \rangle^{2/9}} \langle T_e \rangle^{1/6} G\left[\langle T_e \rangle, \left(\frac{l}{a}\right)\right] \quad \left(\frac{m}{sec}\right) \quad \cdots (7.24)$$

where M = "molecular" weight of fuel (for D_2, M = 4)

f = (# of atoms in the pellet)/(# of ions in the plasma)

f ~ 0.1 - 0.5 is used mostly

f ≳ 1 may disrupt the plasma confinement

V = plasma volume (m^3)

$\langle n \rangle$ = vol. averaged plasma density (m^3)

$\langle T_e \rangle$ " " elect. temp. (eV)

G = function of $\langle T_e \rangle$ and $\left(\frac{l}{a}\right)$ (see figure 25E1)

Dolan; Vol. III, FR

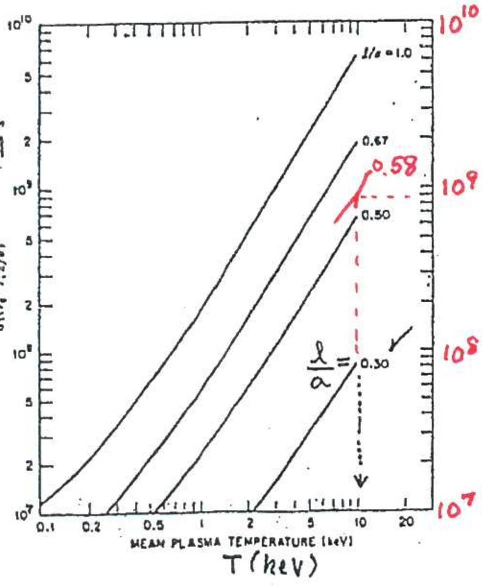

Fig. 25E1. Variation of G with $\langle T_e \rangle$ for various (l/a). From S.L. Milora and C.A. Foster, IEEE Transactions on Plasma Science PS-6, 578-592 (1978), Fig. 6. © 1978 IEEE.

ex. Estimate required deuterium pellet velocity, u, injected into a plasma with

pl. radius, a = 1.3 m

$\langle n \rangle = 10^{20}\ m^{-3}$

V = 300 m^3

$\langle T_e \rangle$ = 10 keV

& f = 0.3

$\frac{r}{a} = 0.7$ desired.

ans. From Fig. 25E1, $\frac{l}{a} = 0.3$, and $G[10, 0.3] = 8 \times 10^7$

Eq. (25E7) → $u = 1.3 \frac{1}{(4)^{1/3}} \frac{1}{(0.3 \times 300)^{5/9}} \frac{1}{(10^{20})^{2/9}} \times (10 \times 10^3)^{1/6} \times (8 \times 10^7) = 924 \frac{m}{sec}$

∴ u = 924 m/sec (for penetration)

Prob. 7.8 If the pellet of the example problem (on the previous page) had $u = 10^4$ m/s, how far could it penetrate? What is its radius?

Given $u = 10^4$ m/s, $a = 1.3$ m, $\langle n \rangle = 10^{20}$ m^{-3}, $V = 300$ m^3, $\langle T_e \rangle = 10$ keV,

f = # of atoms in the pellet / # of ions in the plasma $= 0.3$, M (for D_2) = 4.

Recall $u = a (M)^{-1/3} \cdot (fV)^{-5/9} \cdot \langle n \rangle^{-2/9} \cdot \langle T_e \rangle^{1/6} \cdot G\left[\langle T_e \rangle, \left(\frac{\ell}{a}\right)\right]$

Solve for G, $G\left[\langle T_e \rangle, \left(\frac{\ell}{a}\right)\right] = \dfrac{u M^{1/3} (fV)^{5/9} \langle n \rangle^{2/9}}{a \langle T_e \rangle^{1/6}}$

$$= \frac{(10^4 \text{ m/s})(4)^{1/3} [(0.3)(300 \text{ m}^3)]^{5/9} (10^{20} \text{ m}^{-3})^{2/9}}{(1.3 \text{ m})(10^4 \text{ eV})^{1/6}}$$

$$= 8.92 \times 10^8$$

From this value, along with $\langle T_e \rangle = 10$ keV, using Fig. 25E1 (Dolan, Fusion Research, Vol. III)

$\frac{\ell}{a} \simeq 0.58$

for which the penetration depth would be

$\ell = (0.58)(1.3 \text{ m}) = \boxed{0.754 \text{ m}}$;

n_s = atomic density of the pellet (m^{-3})

For solid hydrogen $n_s = 4.4 \times 10^{28}$ m^{-3}

to determine the pellet radius, $f = \dfrac{\left(\frac{4}{3}\right)\pi r_p^3 n_s}{\langle n \rangle V} \rightarrow r_p = \left[\dfrac{f \langle n \rangle V}{\left(\frac{4}{3}\right)\pi n_s}\right]^{1/3}$

$$\therefore r_p = \left[\frac{(0.3)(10^{20} \text{ m}^{-3})(300 \text{ m}^3)}{(4/3)(\pi)(4.4 \times 10^{28} \text{ m}^{-3})}\right]^{1/3} = \boxed{3.66 \times 10^{-3} \text{ m}}$$ = radius of pellet

iv) ITER Fueling System:

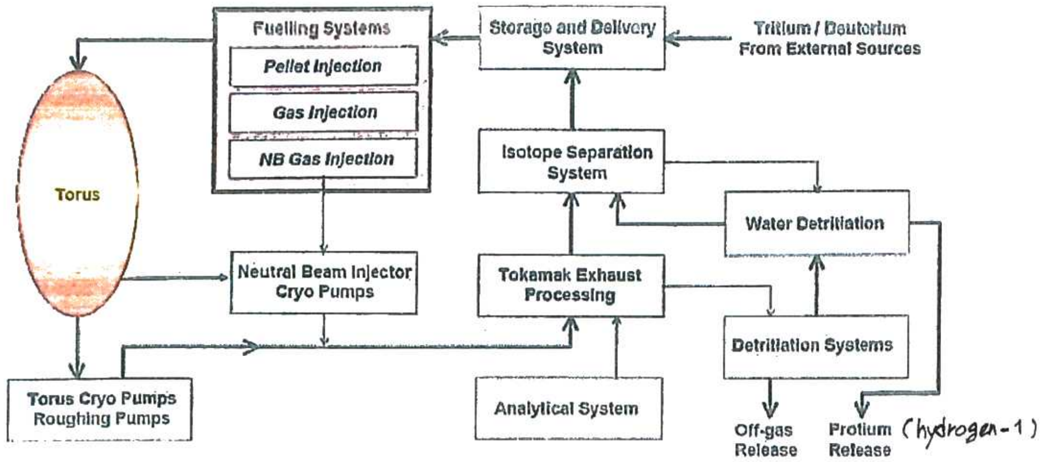

Fig. 7.8 The ITER fueling system. From S. Murayama, KIT Summer School 2008

Fig. 7.9 A twin screw extrusion system for producing solid D_2 pellets. From S. Murayama, KIT Summer School 2008

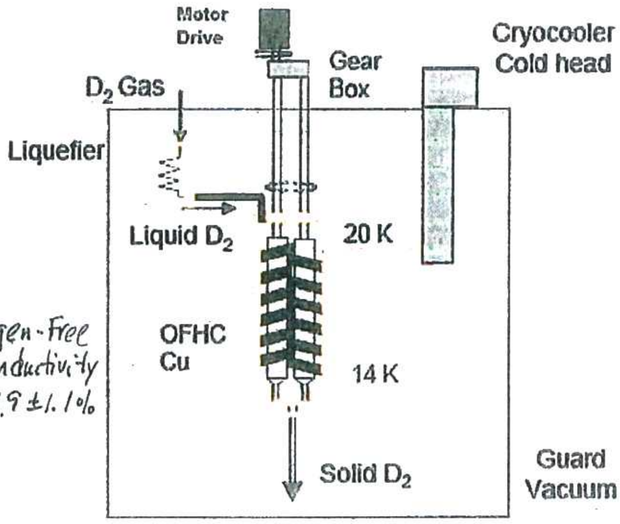

Fig. 7.11 The ITER pellet flight tube. From S. Maruyama, KIT Summer School 2008

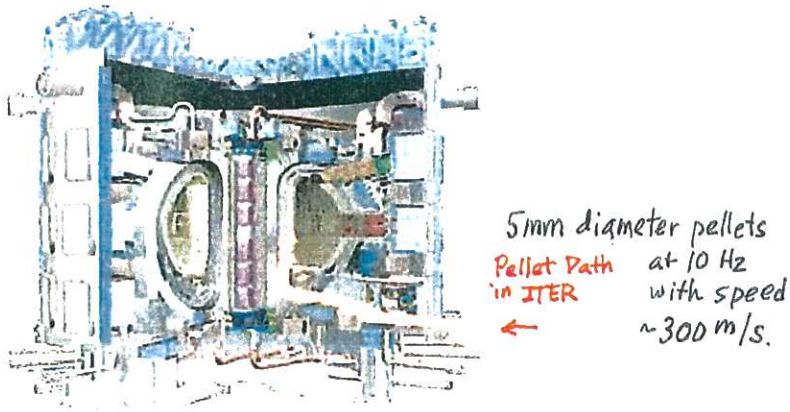

FRT 2, 16 Oct 2019

Table 1.9 Reduction of ITER parameters

	Ignition 1998	"High-Q" 2005
Q	∞ (Ignition)	10
P_f, MW	1,500	400
Burn, s	1,000	400
R/a, m	8.1/2.8	6.2/2.0
I, MA	21	15
B_ϕ, T	5.7	5.3
# TF coils	20	18 → ripple problem

Courtesy of ITER Organization

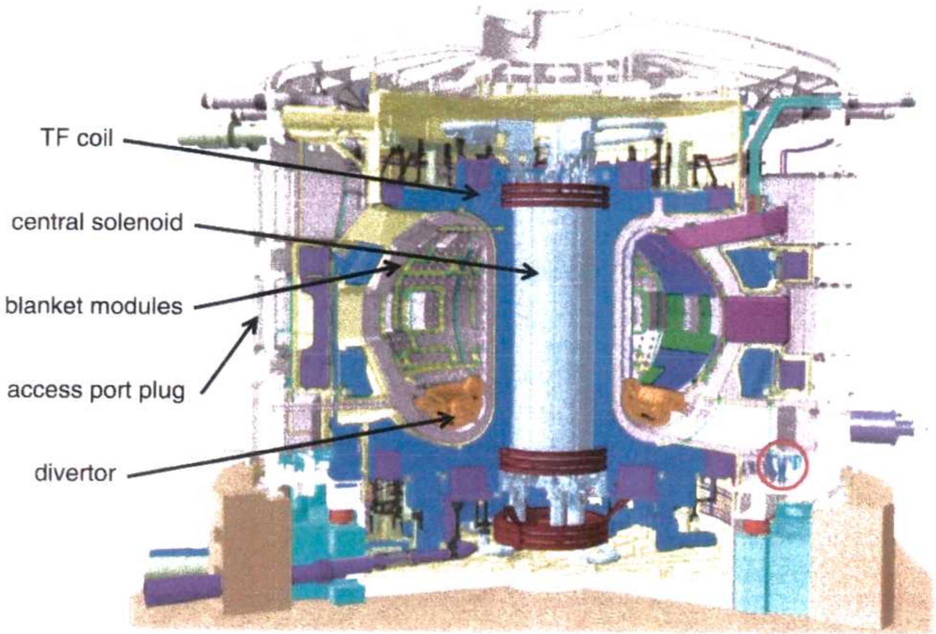

Fig. 1.33 Main components of ITER. A person is shown for scale (in *red circle*). Courtesy of ITER Organization

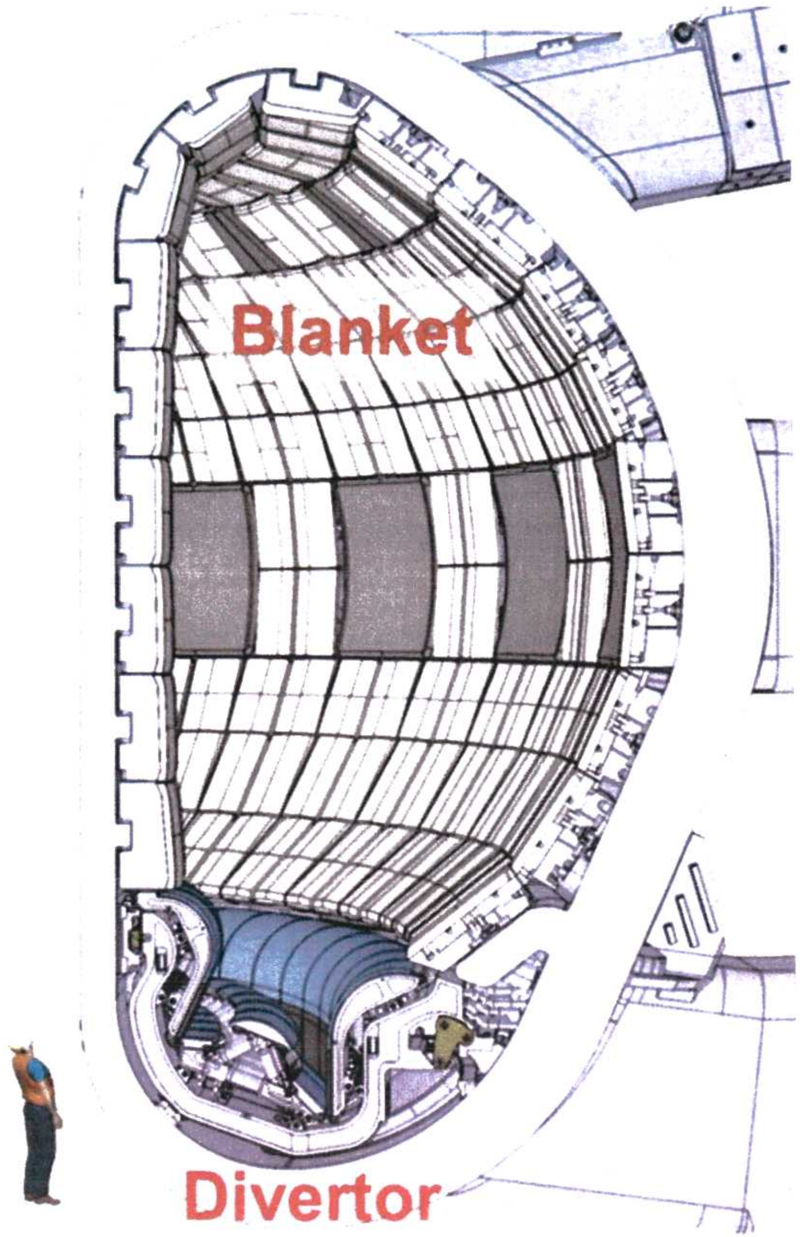

Fig. 2.7 Some of the 440 ITER blanket-shield modules (*rectangular boxes*) and the single-nul divertor (the *W-shaped* region at the *bottom*). Courtesy of ITER Organization

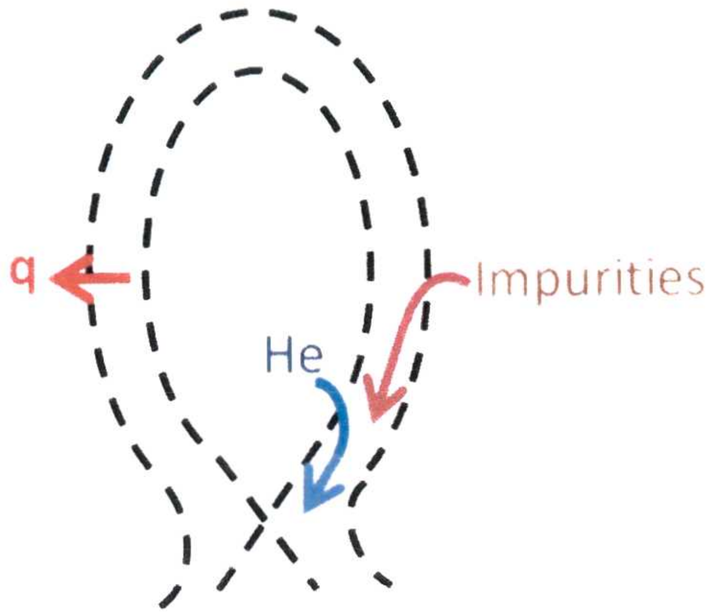

Fig. 7.12 Divertor functions: reduction of heat flux and sputtering of first wall; channeling of helium and sputtered impurities to divertor chamber target below

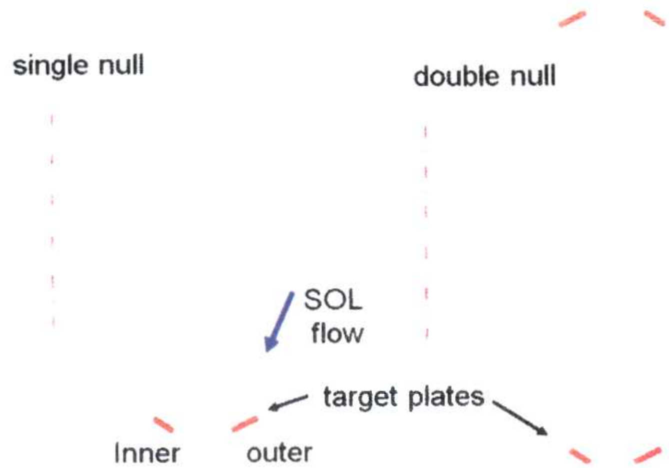

Fig. 7.13 Tokamak poloidal divertors

III. Impurity Control Techniques

i) Divertors (cf. §7.5).

Bend the outer magnetic field lines away from the plasma and lead them to a separate external chamber; thus, the outer layers of plasma are pumped away.

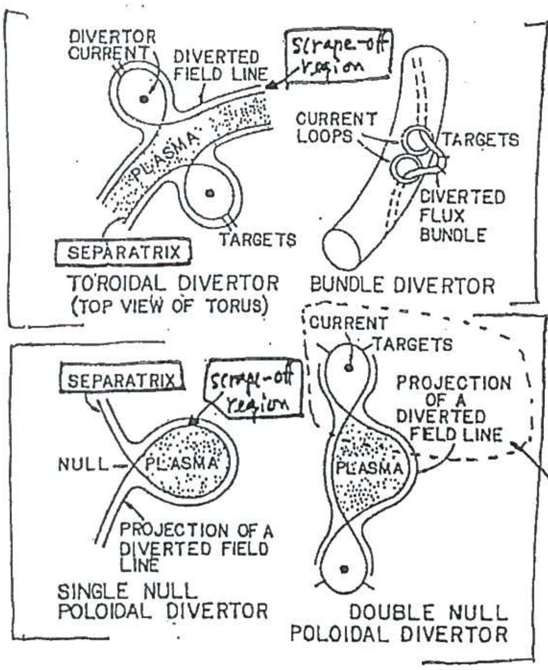

Fig. 25B1. Toroidal, poloidal, and bundle divertors. The poloidal divertor sketches represent cross sections of toruses. (Not all currents shown.) From G.H. Miley, Editor, Proceedings of the First IEEE Minicourse on Fusion, U. of Illinois Fusion Studies Laboratory, 1976, p. 1-34.

← Types of divertors

[See Following Pages]

→ Useful functions:

1) Reduce first wall bombardment by removing plasma from the scrape-off region, thus reducing the sputtering rate.

2) reduce impurity concentration in the central plasma region by removing impurities sputtered off the walls;

3) Divertor cooling w/ Ne or Ar to reduce wall loading via radiative cooling

plasma flow:

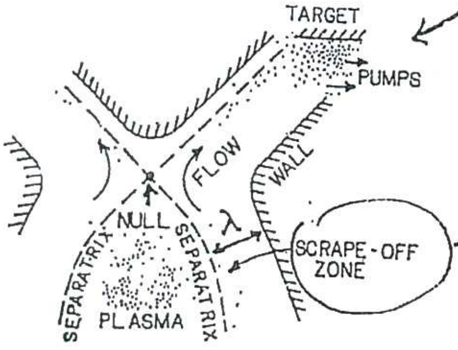

<Upper half of a double-null tokamak poloidal divertor>

$B_t \gg B_p$

At the "Null", $B_p = 0$ but $B_t \neq 0$

→ Let's simplify the scrape-off region by a long straight rectangle.

Fig. Scrape-off region simplified by a long straight rectangle:

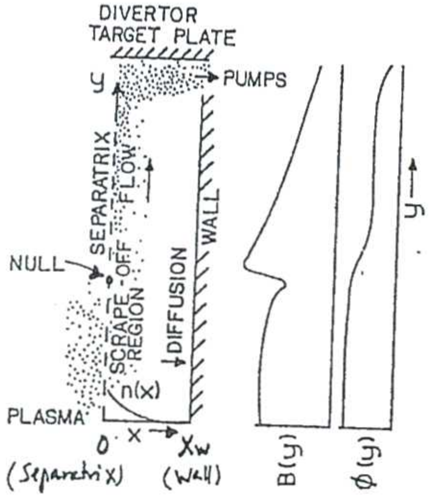

Fig. 25B3. Simplified representation of scrape-off region and flow region (not to scale). The x coordinate represents distance across the magnetic flux surfaces from the separatrix towards the wall, and the y coordinate represents distance along the poloidal flux surfaces towards the target. Typical variations of total magnetic field strength and electrostatic potential in the y direction are shown at the right.

The pcle loss by outflow is equal to

$$\vec{\nabla}\cdot\vec{\Gamma} = \vec{\nabla}_{\parallel}\cdot\vec{\Gamma}_{\parallel} + \vec{\nabla}_{\perp}\cdot\vec{\Gamma}_{\perp} \qquad \left[\vec{\Gamma} = n\vec{u}_i\right] \text{ (ion pcle flux)}$$

$$\simeq \frac{n u_{\parallel}}{L} - \frac{\partial}{\partial x}\left(D_{\perp}\frac{\partial n}{\partial x}\right), \qquad \left(\frac{u_{\parallel}}{L} \simeq \tau_{\parallel}^{-1}\right)$$

where n = ion density

$u_{\parallel}$ = ion parallel flow velocity

$\frac{L}{u_{\parallel}} \equiv \tau_{\parallel}$ $\left[\tau_{\parallel} \approx \frac{L}{c_s}\right.$ (ion sound speed)

$D_{\perp}$ = diffusion coeff.

Note: Particle conservation for ions, $\left(\frac{\partial n_i}{\partial t}\right)$:

$$\frac{\partial n_i}{\partial t} = n_n n_i\langle\sigma_i v_i\rangle + n_n n_e\langle\sigma_e v_e\rangle - n_e n_i\langle\sigma_r v\rangle$$

(n_n: neutral atom density; first two terms: prod^n by ionization; last term: loss by recombination (small))

$$- \vec{\nabla}\cdot(n_i\vec{u}_i) \quad \cdots\cdots (5.D.1)$$

(loss by outflow)

$$\overbrace{\frac{\partial n_i}{\partial t} + \vec{\nabla}\cdot(\overbrace{n_i\vec{u}_i}^{\Gamma})}^{\text{Outflow}} = n_n n_i\langle\sigma_i v_i\rangle + \overbrace{n_n n_e\langle\sigma_e v_e\rangle}^{\text{ionization}} - \overbrace{n_e n_i\langle\sigma_r v\rangle}^{\text{recombination}} \quad \cdots (7.26)$$

$\frac{\partial n_i}{\partial t} + \vec{\nabla}\cdot(n_i\vec{u}_i) \simeq \frac{n_i}{\tau_{\parallel}} - \frac{d}{dx}\left(D_{\perp}\frac{dn_i}{dx}\right)$

$n_n n_i\langle\sigma_i v_i\rangle \sim 0$ ($\because$ low scrape-off plasma temp. not causing much ion^n by ions)

$[n_i = n_e \equiv n]$

$$\Rightarrow \boxed{\frac{n}{\tau_{\parallel}} - \frac{d}{dx}\left(D_{\perp}\frac{dn}{dx}\right) = n_n n\langle\sigma_e v_e\rangle - n^2\langle\sigma_r v\rangle}$$

[Note: $\underbrace{D_{\text{neo-classical}}}_{\text{minimum diffusion coef}} < D_{\perp} \lesssim \underbrace{D_{\text{Bohm}}}_{\text{maximum diffusion coeff.}}$]

$$\frac{n}{\tau_{\parallel}} - \frac{d}{dx}\left(D_{\perp} \frac{dn}{dx}\right) = n n_n \langle \sigma_e v_e \rangle - n^2 \langle \sigma_r v \rangle \quad \text{----}(*)$$

Assume: $D_{\perp} \simeq$ constant

$\langle \sigma_r v \rangle \simeq 0$, i.e., recombination is negligible.

Then, eq. above (*) becomes

$$\frac{n}{\tau_{\parallel}} - D_{\perp} \frac{d^2 n}{dx^2} \simeq n n_n \langle \sigma_e v_e \rangle$$

$$\Rightarrow \quad \boxed{\frac{d^2 n}{dx^2} = \frac{n}{D_{\perp}}\left(\frac{1}{\tau_{\parallel}} - n_n \langle \sigma_e v_e \rangle\right) \equiv \frac{n}{\lambda^2}} \quad \cdots (7.28)$$

$$\text{where } \lambda^2 \equiv D_{\perp} \tau_{\parallel} \left(1 - n_n \langle \sigma_e v_e \rangle \tau_{\parallel}\right)^{-1} \quad \cdots (7.29)$$

[$\lambda \equiv$ <u>thickness</u> of scrape-off region]

If λ = constant, $n(0) = n_0$ at $x = 0$ (at the separatrix)

$n(x_w) \simeq 0$ at $x = x_w$ (at the walls),

and $\lambda \ll x_w$, then $\boxed{n(x) = n_0 e^{-x/\lambda}}$ $\cdots (7.30)$

Note: For large x_w, the thickness of plasma density profile, eq. (7.28) and (7.30), is ~ equal to λ.

→ a thick plasma is more effective than a thin plasma in ionizing wall-generated impurity atoms before they reach the separatrix.

→ plasma is thinnest if $n_n \langle \sigma_e v_e \rangle \simeq 0$ (no ionization by e^-'s) from eq. (7.29).

[Note: Example 25B1 (Dolan, Vol. III) for plasma thickness in scrape-off region, λ for deuterium plasma: Consider [1] case I

For $n_0 = 10^{19}\, m^{-3}$, $n_n = 10^{17}\, m^{-3}$, $L = 100\, m$, $T_e = 0.3\, keV$, $T_i = 1\, keV$, $x_w = 0.5\, m$ and $B = 4T$, $\lambda \simeq 0.07\, m = 7\, cm$]

[Note: Bohm diffusion. $D_B = T_e / 16eB$] [Eq. (7.29)]

[Also, See Example 7.4]

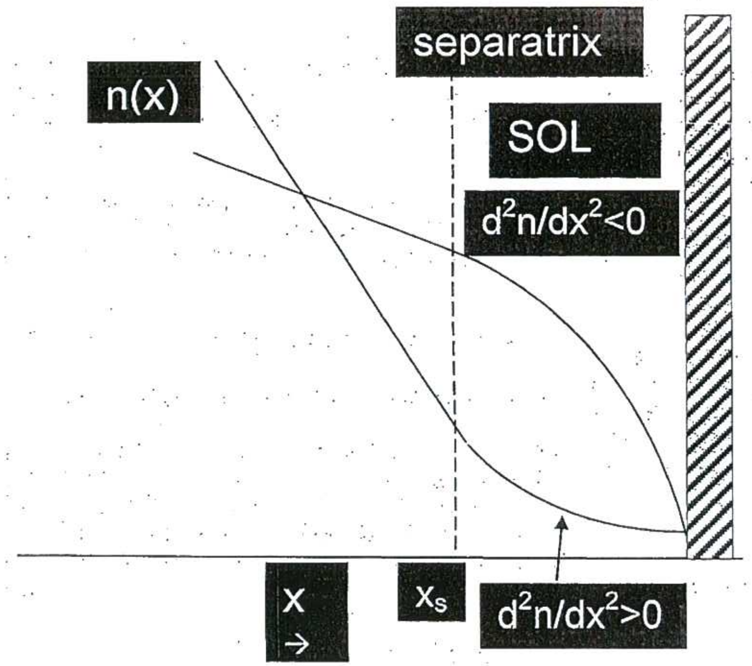

Figure 7.16. Density profile in the SOL. [Dolan 2011]
(Scrape-of-Layer)

If ionization dominant, then

$$d^2n/dx^2 < 0 .$$

The curvature is concave downwards and dn/dx is not steep at the separatrix.

If ionization negligible, then the curvature is upwards, and the density decays roughly exponentially away from the separatrix,

$$n = n_s \exp(-(x-x_s)/\lambda) .$$

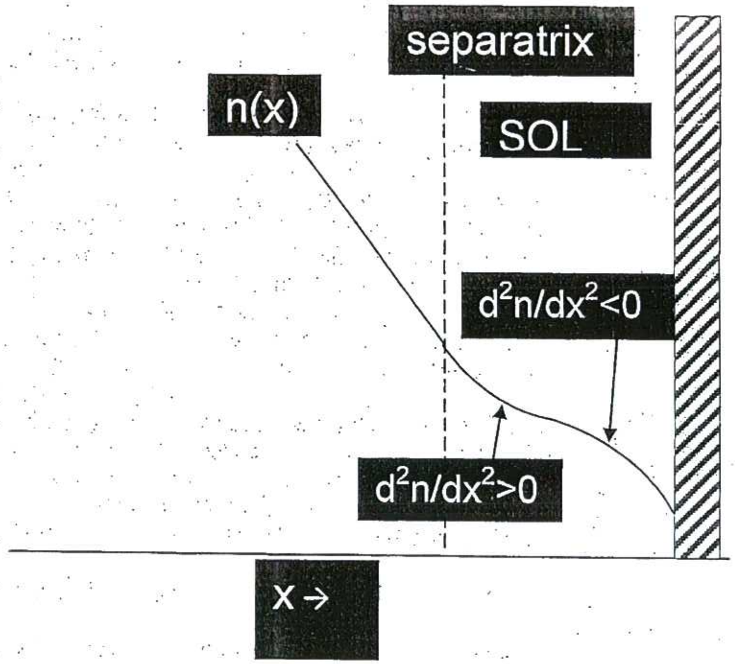

Figure 7.17. A case where ionization is dominant near the wall, but transport is dominant near the separatrix. [Dolan 2011]

Recombination may also be significant in places where n is very high, such as near the target.

Most of the impurities coming from the first wall are also ionized in the SOL and channeled to the divertor so that they do not reach the core plasma.

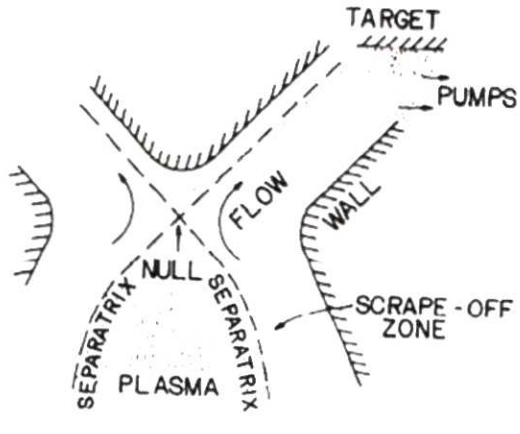

Fig. 7.14 The *upper half* of a double-null tokamak poloidal divertor (coils not shown). Plasma crossing the separatrix may flow along the B field to the target, or may diffuse across the B field to the walls

The approximate variations of plasma density, temperature, and neutral density along the magnetic field from the separatrix to the divertor target are illustrated in Fig. 7.15.

The plasma cools by radiation as it flows from the x-point (separatrix) to the divertor target, especially if impurities like argon are injected into the SOL.

For a simplified analysis of plasma flow in the SOL, we use the following definitions:

$$\begin{aligned}\tau_{\|} &\approx \text{sum of time delays for flow to target or limiter}\\ &\approx (\text{ambipolar flow along B}) + (\text{mirror detrapping})\\ &\quad + (\text{electrostatic potential detrapping})\end{aligned}$$

$$\tau_{\|} \approx L/c_s + F(\tau_i, R_m, \phi(x)),$$

where $c_s \approx [(T_e + 1.7\,T_i)/m_i]^{1/2}$ is the ion sound speed,

L Flow path length

τ_i Ion collision time

ϕ Electrostatic potential

R_m Magnetic mirror ratio along B

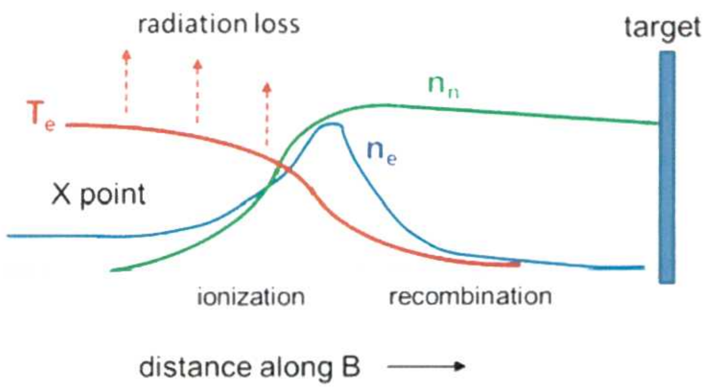

Fig. 7.15 Variations of plasma density, electron temperature, and neutral density along the magnetic field in the divertor channel, showing where ionization and recombination are dominant (Based on drawing of Asakura et al. 2010)

Nucl. Fusion, 19 (1979) p. 889

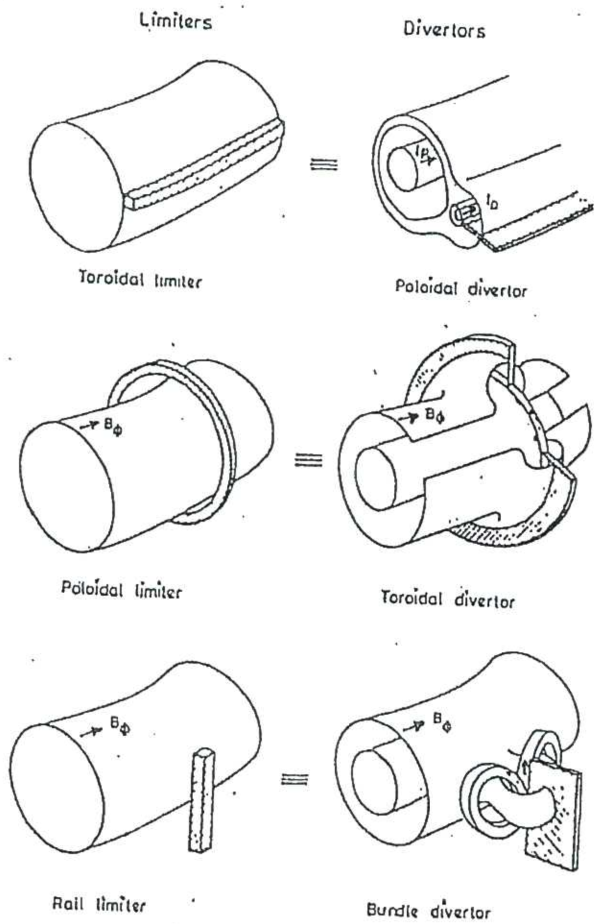

FIG. 98. Comparison between various limiter and divertor configurations.

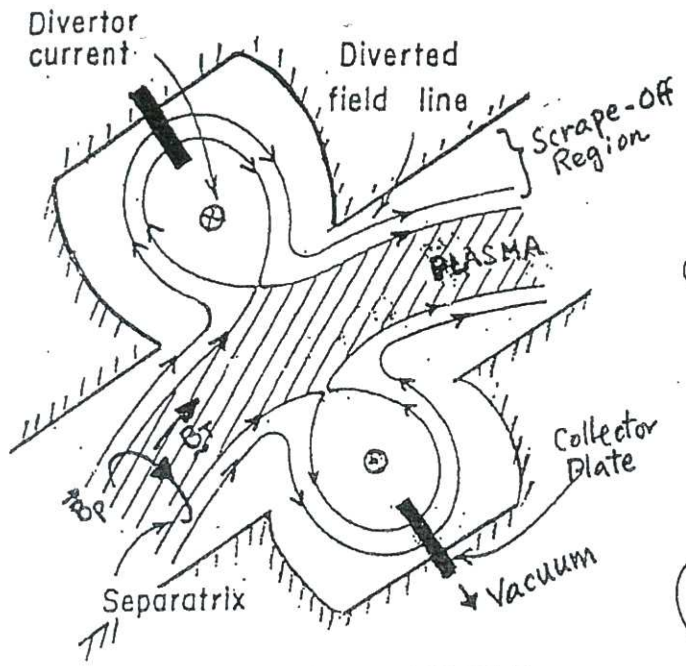

TOROIDAL DIVERTOR

(Top view of torus)

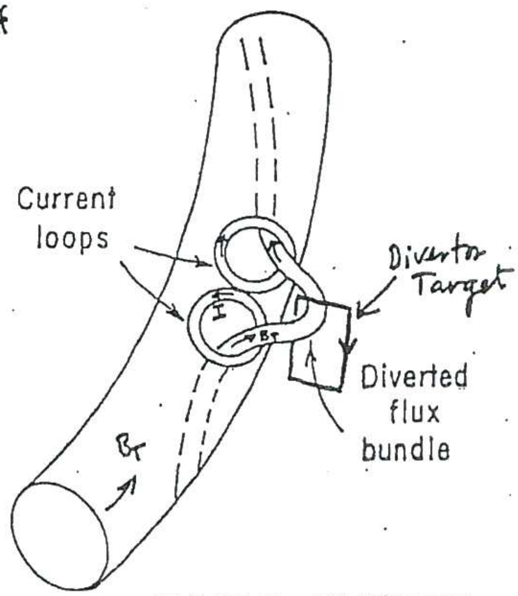

BUNDLE DIVERTOR

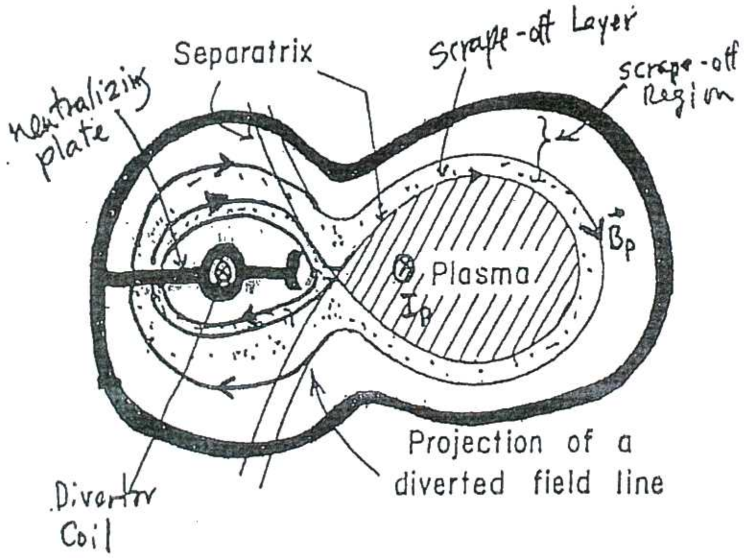

SINGLE NEUTRAL POINT

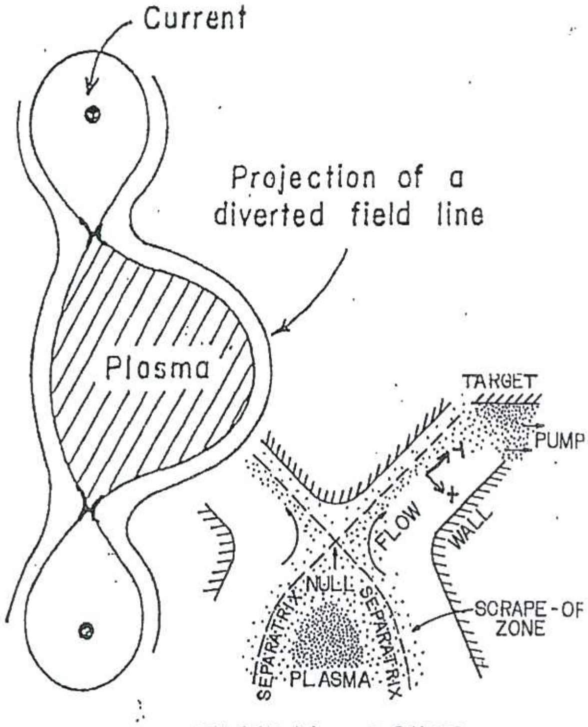

DOUBLE NEUTRAL POINT

(Not all currents shown)

POLOIDAL DIVERTOR

(CROSS-SECTION OF TORUS)

tokamak divertors

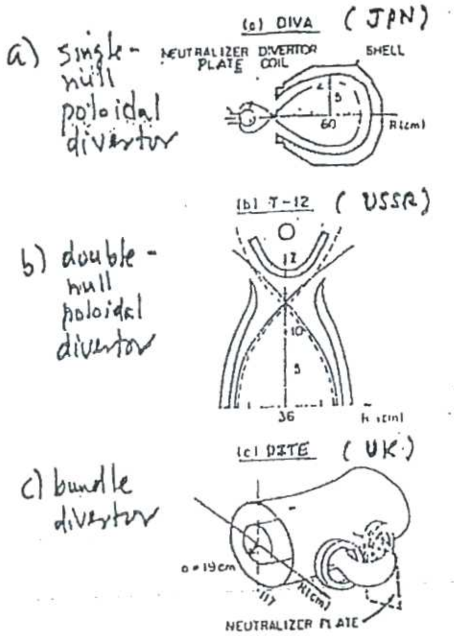

Fig. 25B4. Tokamak divertors. (a) the DIVA single-null poloidal divertor, (b) the T-12 double-null poloidal divertor, (c) the DITE bundle divertor. From Shimomura and H. Maeda, "Divertor experiments for controlling plasma-wall interactions", Journal of Nuclear Materials 76 & 77, 45-48 (1978), Fig. 1.

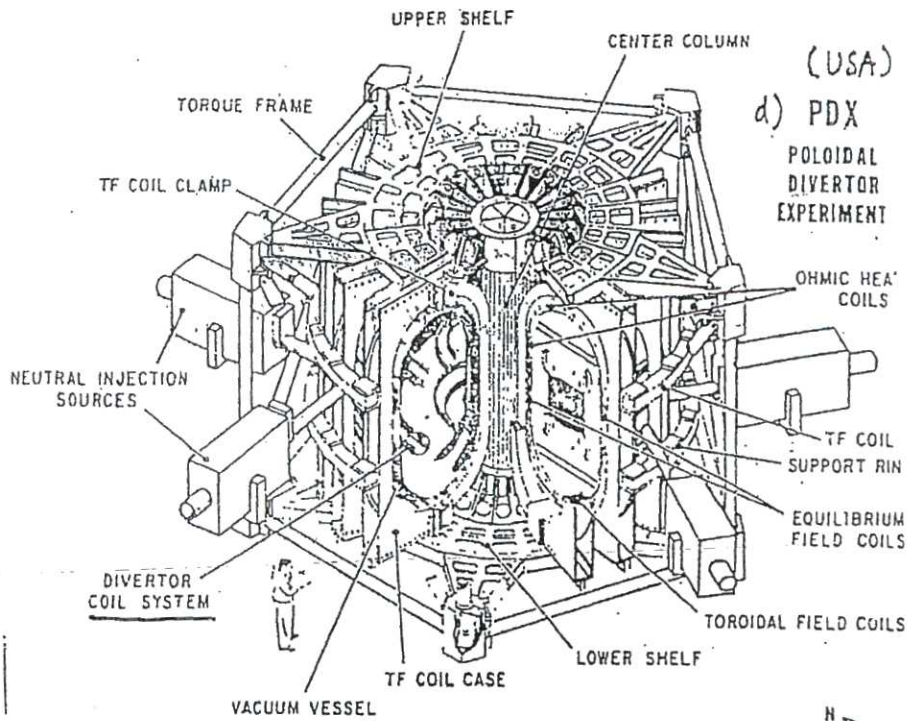

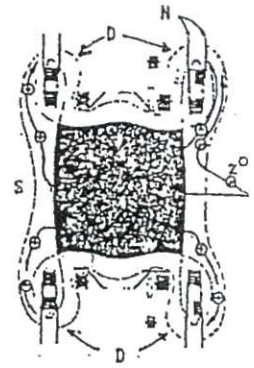

Fig. 25B5. The Poloidal Divertor Experiment (above) and a cross section of the divertor region (right).
N = neutralizer plates
D = divertor region
S = scrape-off region
z^0 = sputtered impurity atom

Courtesy of PPPL.

Table 25B1. Parameters of PDX, with divertor operating.

minor radius	a	0.47 m
major radius	R	1.45 m
toroidal field	B_t	2.4 T
plasma current	I_p	0.5 MA
plasma temperature	T	
0.3 MW ohmic heating		1-2 keV
6 MW neutral beams for 0.5 s		2-6 keV
plasma density	n	$0.4\text{-}3\times10^{20}$ m^{-3}
plasma beta	β	2-5 %
energy confinement time	τ_E	0.1 s

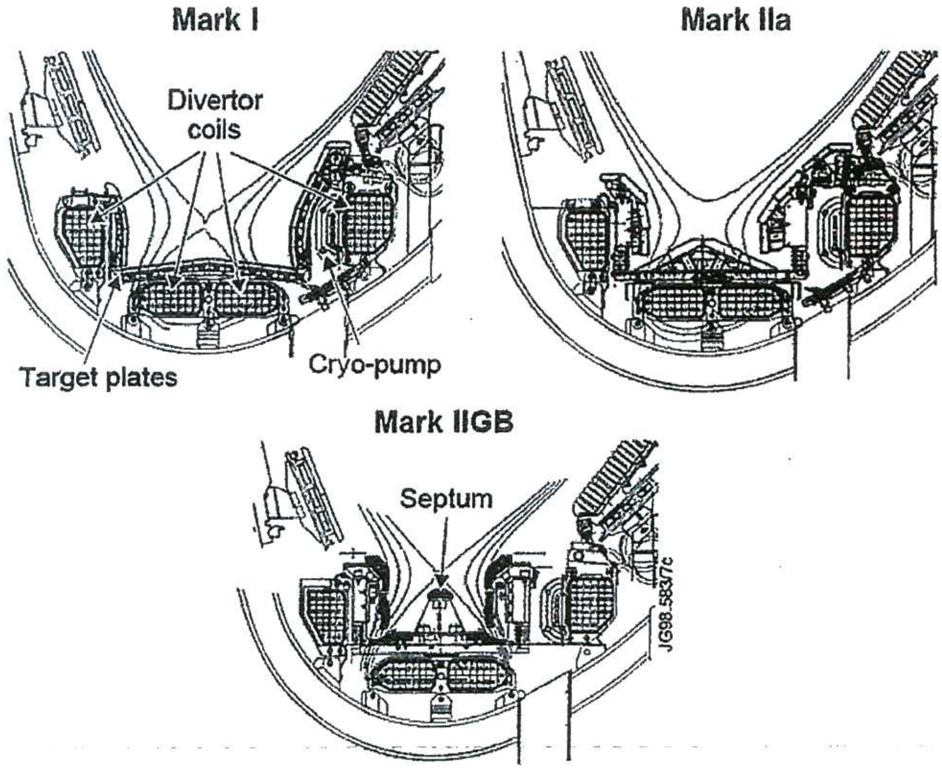

Fig. 7.19 Greater closure of the JETdivertor as it was changed from the Mark I → Mark IIA/P → Mark IIGB (JET Team 1999, Fig. 1). Copyright 1999, International Atomic Energy Agency

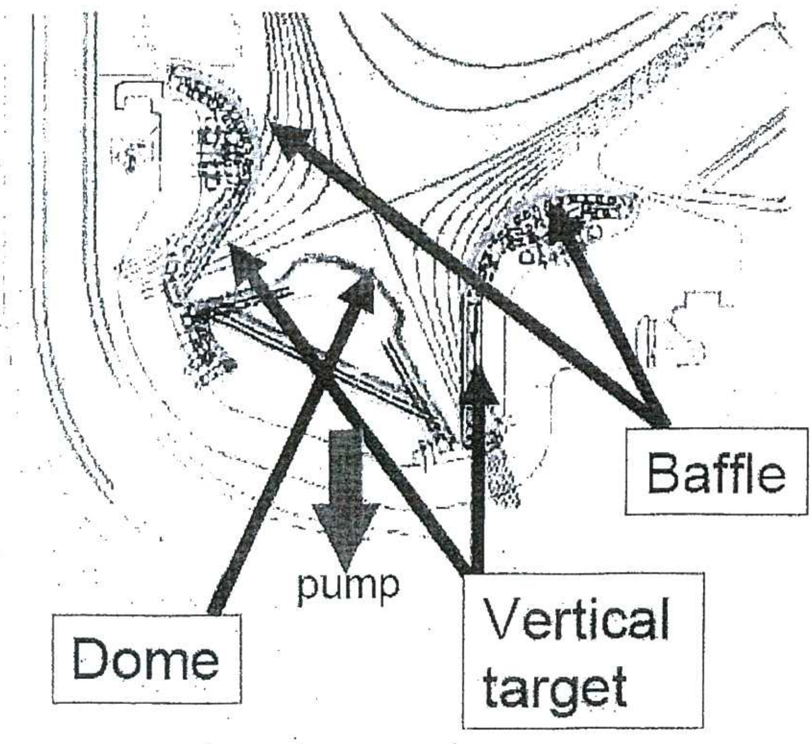

Figure 7.22. The ITER divertor. From T. Ihli, FZK Summer School, 2008.

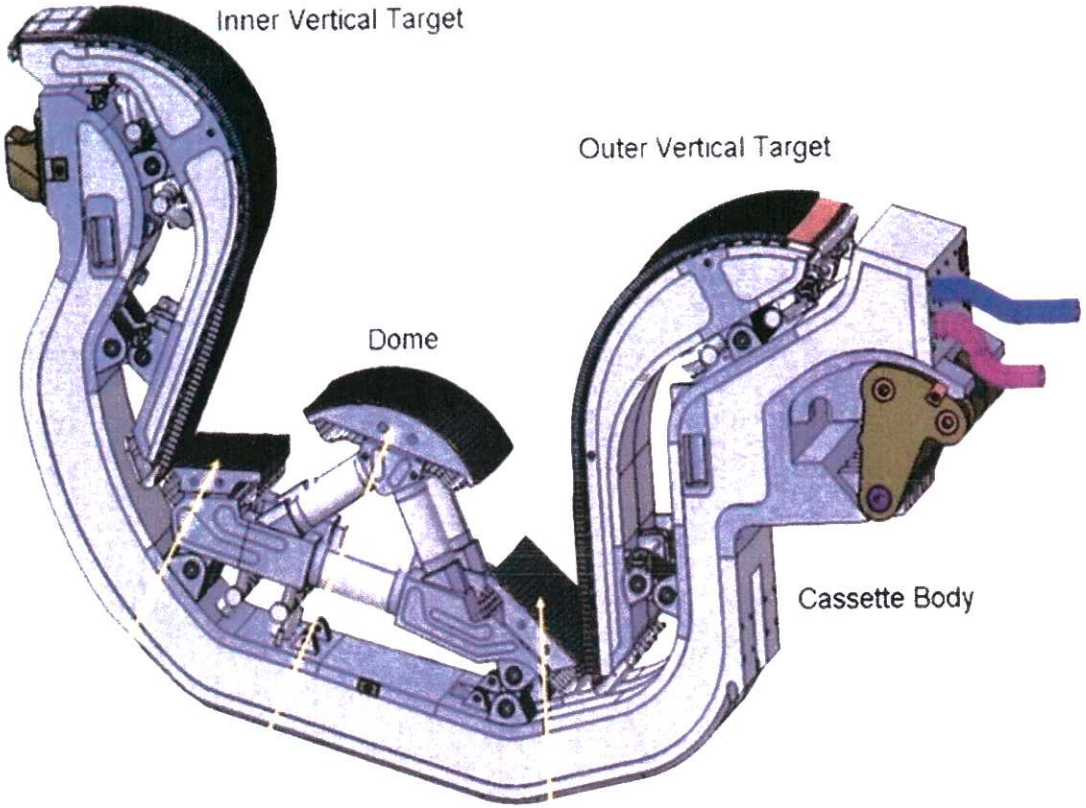

Fig. 2.10 An ITER divertor cassette. The plasma-facing materials in the dome and targets will be water-cooled tiles with tungsten surfaces. Courtesy of ITER Organization

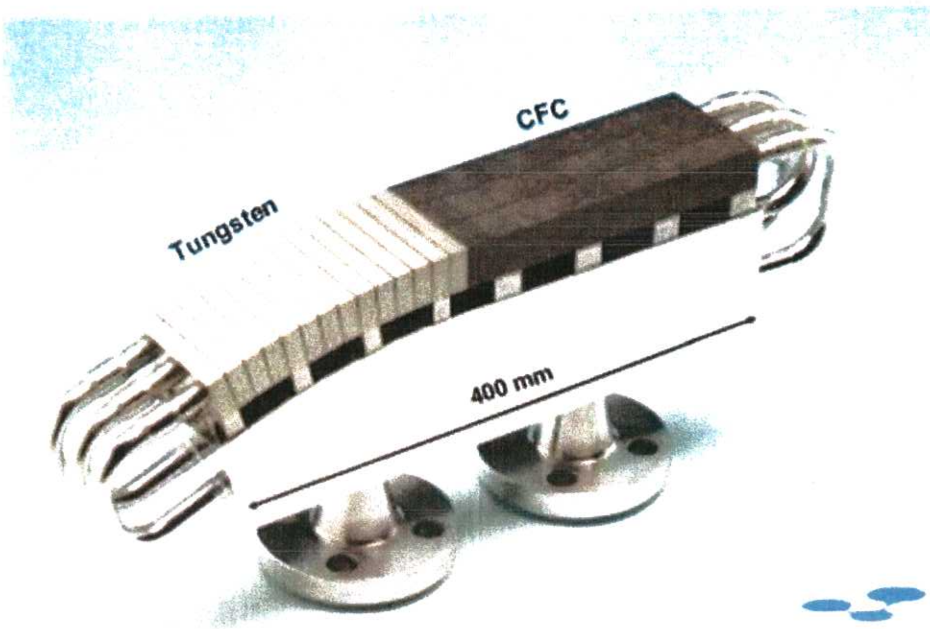

Fig. 2.8 Armor tiles of W and C bonded to copper substrate containing stainless steel coolaı tube (Merola 2008)

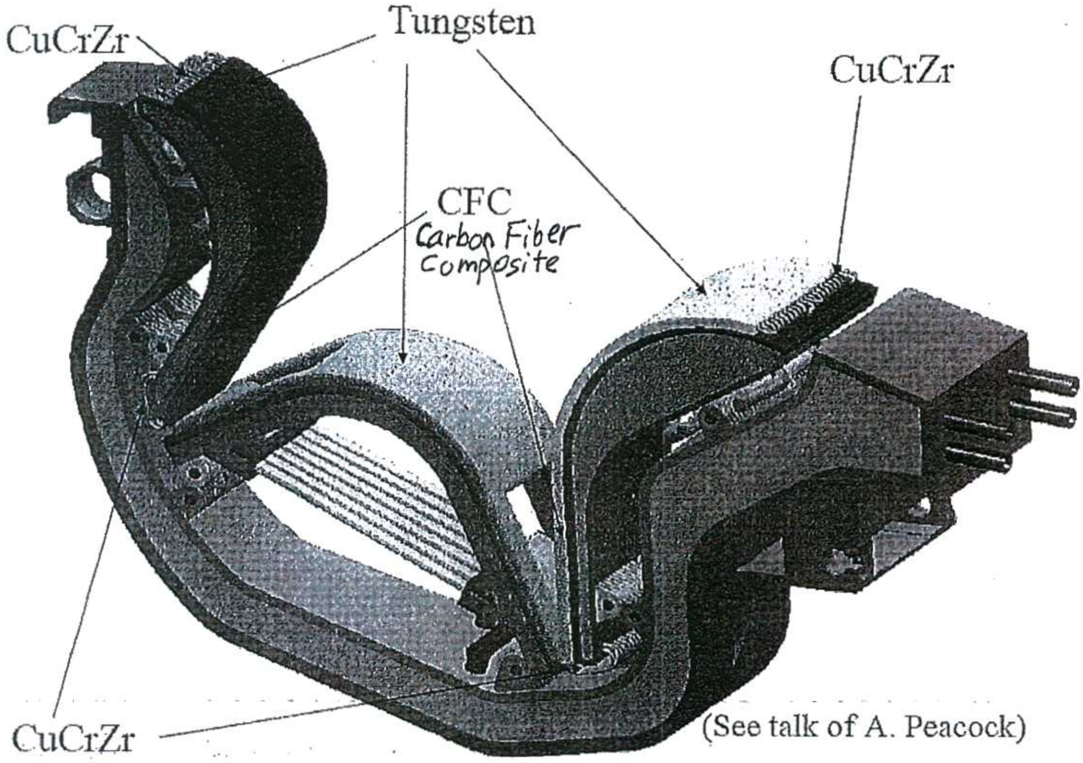

Figure 7.20. Possible cooling water tube arrangement for ITER. Blue tubes are cool inflow and red are hot outflow. From T. Ihli, FZK Summer School, 2008.

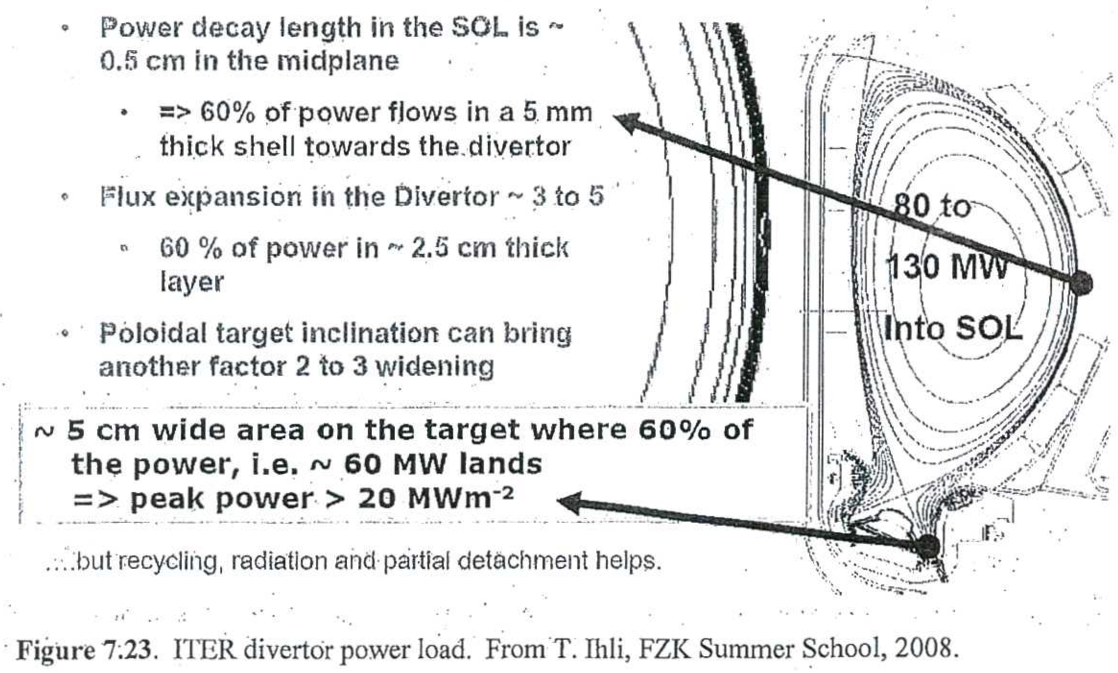

Figure 7.23. ITER divertor power load. From T. Ihli, FZK Summer School, 2008.

The heat flux at the divertor is reduced by expansion of the magnetic flux surfaces and by tilting the target relative to the field lines. This divertor must be able to handle a variety of events, Snowflake Divertors

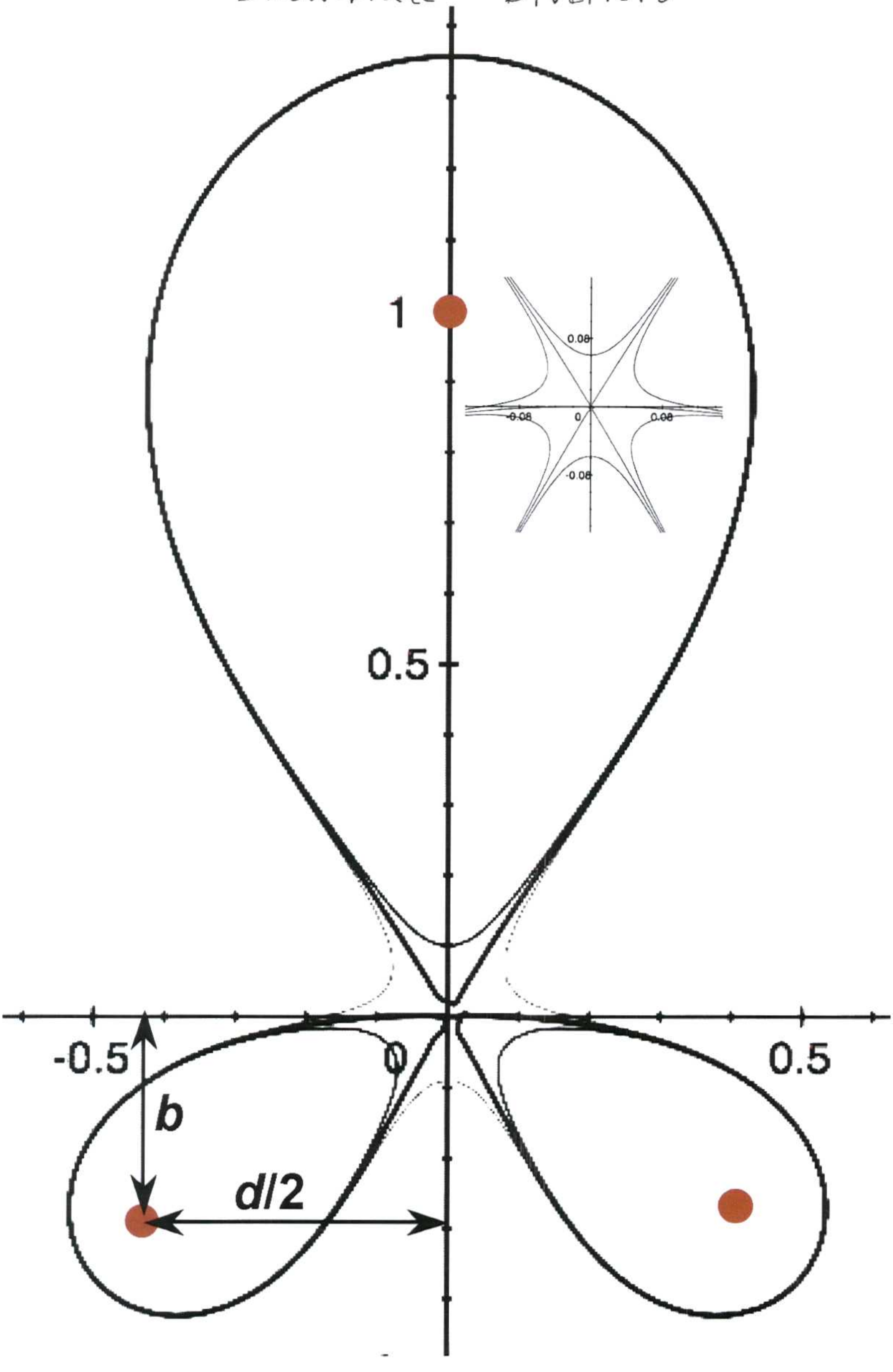

Snowflake Divertors

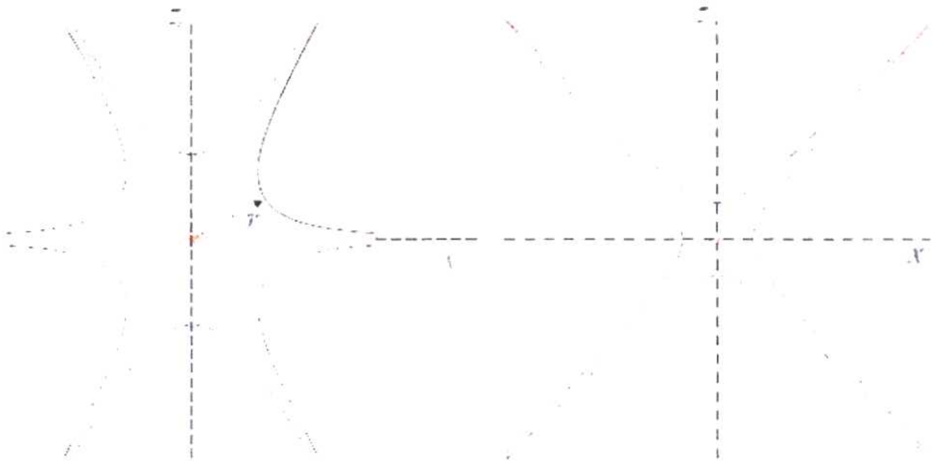

Figure 1. The shape of separatrix in the vicinity of the PF null for the SF divertor (left) and standard divertor (right). Shown by a bold red line is a separatrix; thin line represents an adjacent flux surface. The confinement region is in both cases situated in a sector pointing upward. Note that in the case of a SF there are four branches of the separatrix pointing away from the confinement zone, so that one can have four strike points in the divertor.

Fig. 7.35 Comparison of the SOL in a snowflake divertor (*lines 1, 2*) with the SOL in an X-point divertor (*lines 3, 4*) (Ryutov 2007)

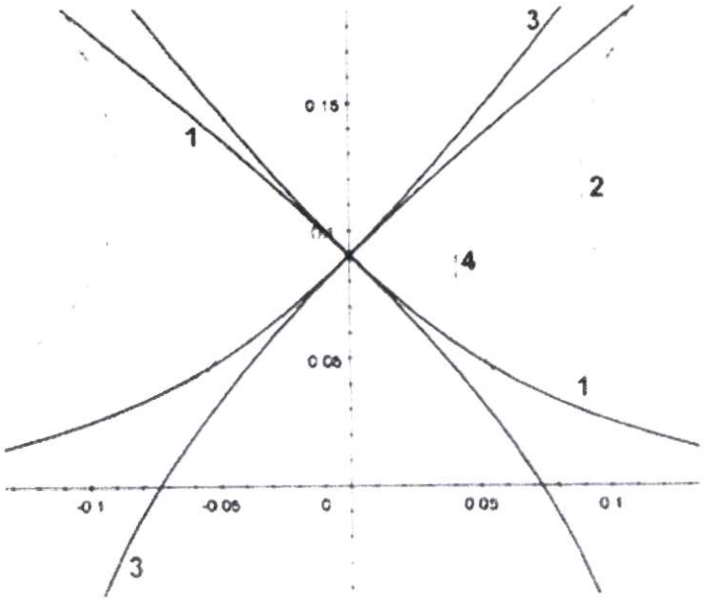

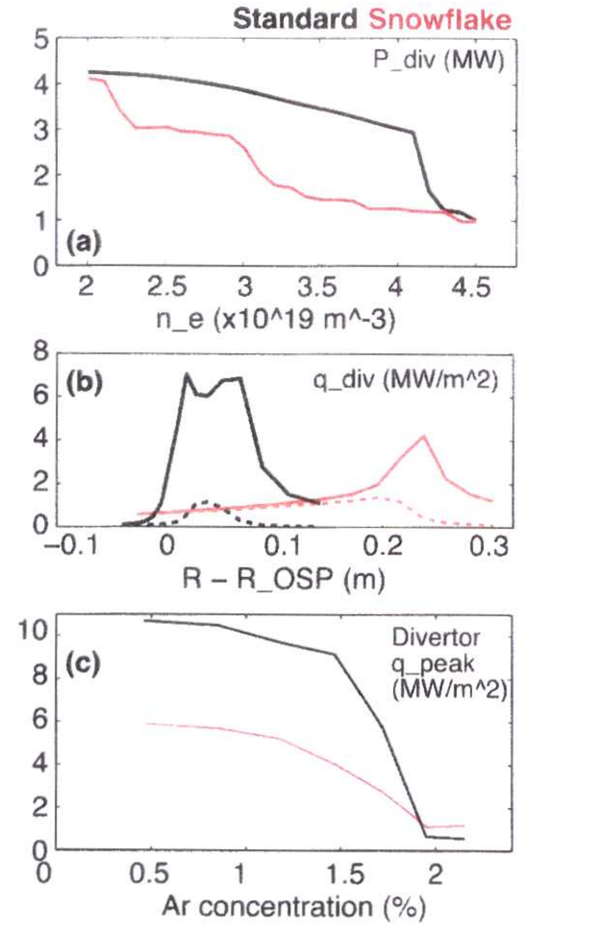

Fig. 14. UEDGE modeling results for NSTX-U standard (black traces) and SF-minus (red traces) divertor configurations. (a) Divertor power as a function of electron density (n_e at the core-boundary interface). (b) Divertor heat flux profiles at $n_e = 3.5 \times 10^{-19}$ m^{-3}—total (including the radiative heating, solid lines) and without the radiative heating flux (dashed lines). (c) Peak divertor heat flux (total, including the radiative heat flux) as a function of argon concentration in a radiative argon-seeded divertor. [Soukhanovskii (2016)]

Swirling Liquid Lithium Wall Concept:

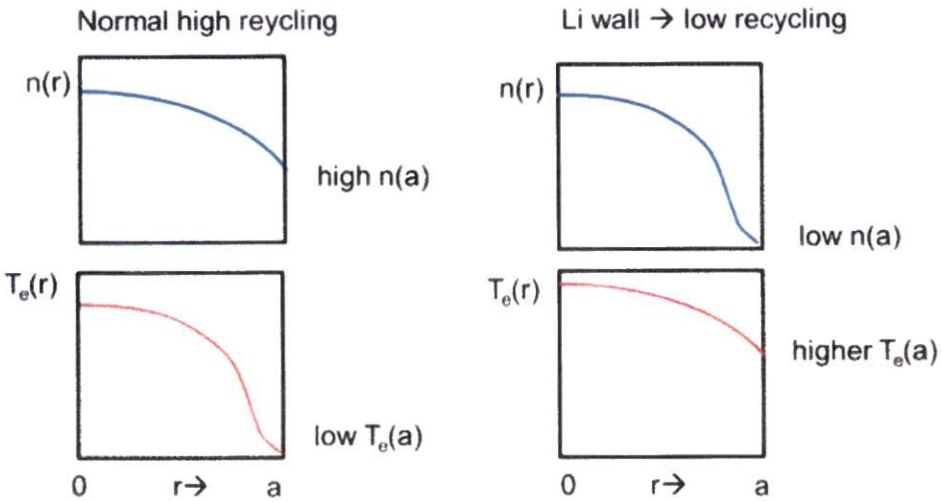

Fig. 7.39 Effect of recycling on density and temperature profiles. High recycling lowers edge temperature and requires more heating (These profiles are simplified for clarity. There will usually be other features, such as an edge pedestal)

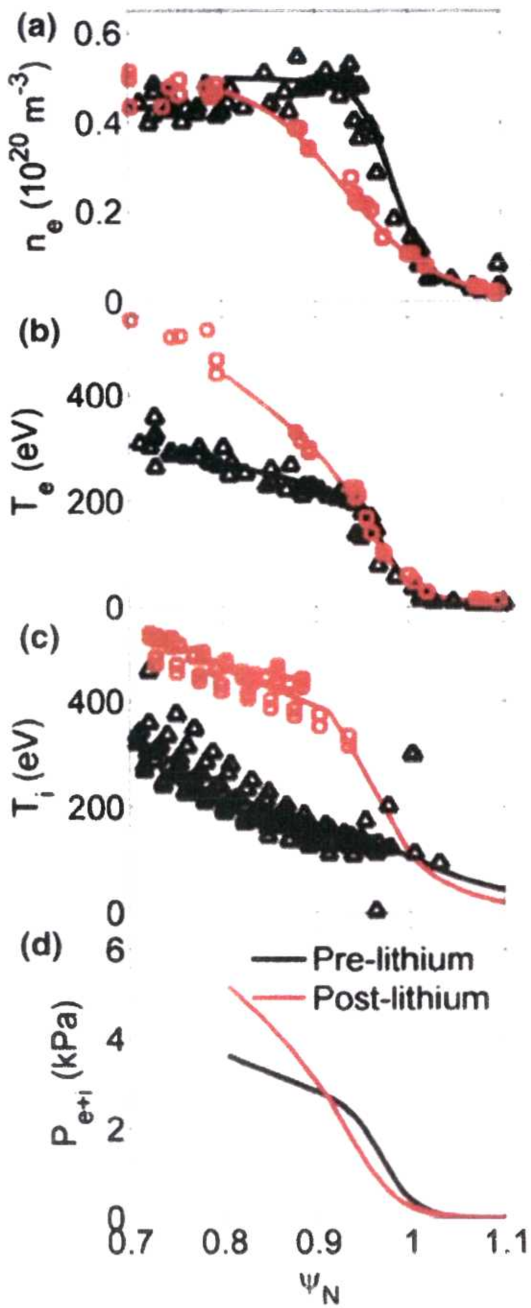

Fig. 7.40 Profiles of density, temperatures, and pressure in NSTX without Li walls (*black triangles*) and with Li walls (*red squares*) (Canik 2011)

Divertor Pumping requirements

Divertor's typical loads ~ MW/m^2

↑ concern w/ overheat of the divertor

ex. For a fusion reactor with

1) 200 MW of heat flowing into the divertor, (half of energy carried by ions)
2) $100\ m^2$ total target area
3) average p'cle energy ($\langle W_i \rangle$) being 50 eV
4) $T_{target\ \&\ wall}$ being 800 °K,

estimate the required pumping speed and cryopanel area to keep the target region at $p = 0.1$ Pa (8×10^{-4} torr).

ans. Required ion flow rate,

$$\dot{N}_i = \frac{P_i}{\langle W_i \rangle} = \frac{200\ MW/2}{50\ eV} = \frac{1 \times 10^8\ J/sec}{50 \times 1.6 \times 10^{-19}\ J/ion} = 1.25 \times 10^{25}\ \frac{ions}{sec}$$

Eq. (19B6) → $\dot{N} = \frac{Q}{kT_i}$, [Q = throughput [Pa-m³/sec], "energy flow rate"]

$$\Rightarrow Q = \dot{N} kT$$
$$= 1.25 \times 10^{25}\ \frac{ions}{sec} \times (1.3807 \times 10^{-23}\ J/°K) \times (800\ °K)$$
$$= 1.38 \times 10^5\ J/sec$$

To find the cryopanel area:

Throughput, $Q = \frac{S_t C}{(S_t + C)} (P - P_u)$

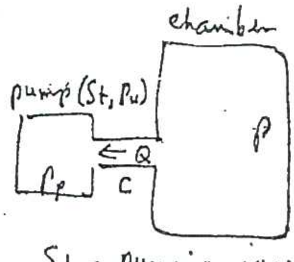

For $P_u \ll p$ & $C \gg S_t$ (large conductance since cryopumps are very close to target plates) → $Q \simeq S_t\, p$

S_t = pumping speed [m³/sec]
C = conductance of tube [m³/sec]

$$\therefore S_t = \frac{Q}{p} = \frac{1.38 \times 10^5}{0.1} = 1.38 \times 10^6\ \frac{m^3}{sec} \quad \text{— ①}$$

But, eq. (9.31) gives $S_t \simeq 89\, A\, (T/300)^{1/2}$ ($\frac{m^3}{sec}$) (T in °K)

$$= 89\, A\, (800/300)^{1/2} = 145.3\, A \quad \text{— ②}$$

From ① & ②

$$\therefore A = 1.38 \times 10^6 / 145.3 = \boxed{9.49 \times 10^3\ m^2}$$! Tough!

III. Impurity Control Techniques (Cont'd)

ii) Neutral Gas Blankets (§7.7.2)

Introduce <u>cold</u> neutral gas around the outside of plasma which will form a <u>cool</u>, <u>high-density</u> plasma layer → neutral gas blanket (or cool plasma blanket)

For L (layer thickness) ~ 0.1 m,
n_n (neut. gas density) $\gtrsim 3\times10^{20}\ m^{-3}$ is needed to make the plasma layer impermeable

[note: $nL \gg 3\times10^{18}\ m^{-2}$ (*) for impermeable condition]

(*) B. Lehnert, Nuclear Fusion 13, 781 (1973).

At wall temperature of 500°K, this density ⇝ $p = n_n kT$

$= (3\times10^{20}\ m^{-3}) \times (1.38\times10^{-23}\ J/°K)(500°K)$

$= \underline{2.07\ Pa}$ (or $2.07\ Pa \times 7.5\times10^{-3}\ \frac{Torr}{Pa}$

$= 0.0155$ Torr

$= \underline{15.5\ mTorr}$)

[1 atm = 1.013×10^{5} Pa
1 bar = 10^{5} Pa ≃ 1 atm
1 Pa = 7.50×10^{-3} torr]

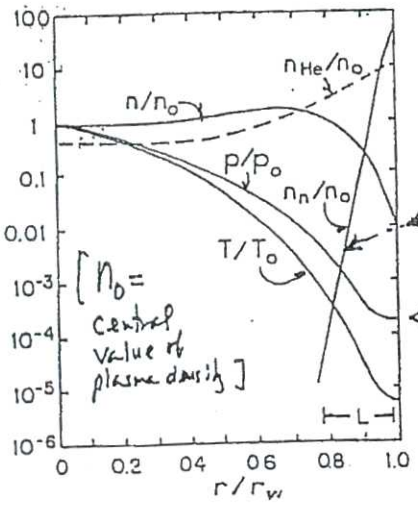

Fig. 7.38

Fig. 25C1. Hypothetical radial variations of plasma density, helium density, pressure, temperature, and neutral gas density n_n, (relative to the central values of plasma density n_0, temperature T_0, and pressure p_0) for the neutral gas blanket concept. The thickness of the "impermeable" edge layer is indicated by L.

<u>Advantages</u>:
- reduced sputtering
- " impurity penetration
- minimum He-density in plasma core

<u>problems</u>:
- possible plasma instability
- high density → high pressure
- incompatible w/ neutral beam heating.

iii) pumped limiters (§7.7.1)

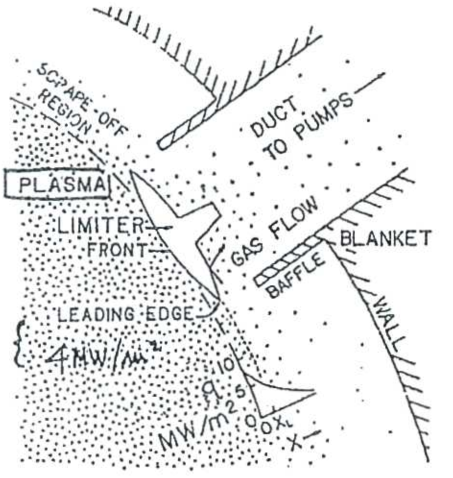

Fig. 7.37
Fig. 25D1. A pumped limiter for impurity control in a tokamak reactor. "[illegible]eading edge" is set back to a [illegible] flux q = 4 MW/m². The vacuum duct may be zig-zagged (not shown) to reduce neutron streaming.

Used for STARFIRE commercial tokamak reactor study.

The distance the pcle travelled,

$$L = 2\pi R \left(\frac{q}{2}\right),$$

where $R = 7$ m (major radius)
$q = 3.6$ (safety factor)
and $L = 80$ m
for STARFIRE design.

Typical scrape-off thickness,
$\lambda \sim 7$ cm.

iv) impurity injection (§7.7.3)
add low-Z (e.g. Ne) to enhance radiation cooling of the edge regions.

v) gas flow.
usually hydrogen moves outwards; impurities inwards — tries to change this flow by injecting hydrogen gas called impurity flow reversal.

vi) neutral beam injection
inject in the direction of plasma current (co-injection) for better confinement and heating, and thus tries to induce impurity flow "reversal."